

Response to major revisions on “ATAT 1.1, an Automated Timing Accordance Tool for comparing ice-sheet model output with geochronological data”

Reviewers comments are in italics. Previous responses and extracts from the manuscript are in quotation marks with bold and italic font. Line numbers refer to track-changes document.

Editors comments to the Authors:

Dear Jeremy Ely and co-authors,

We have now received two further reviews on your manuscript. To my reading, there is one major issue left after this second round, raised by reviewer #2, regarding structural uncertainty. However, the comment by reviewer #1 about the ease of use and the (partial) lack in documentation should be addressed equally. Ideally, the software should be widely usable by the community, but the comment by reviewer #1 indicates it is not so right now.

Please provide a response to all issues raised for the next stage of the process.

With best wishes,

Didier Roche

We would like to thank the editor for his handling of the manuscript and the two reviewers for providing reviews. These have led to improvements to the manuscript.

Reviewer #2 is concerned that we do not deal with uncertainty in our manuscript. The tool has always addressed data-based uncertainty, but we have further clarified this in the manuscript (Lines 456-458). To avoid confusion over nomenclature, we have explicitly defined three sources of model-based uncertainty (see response to reviewer and lines 191-192). ATAT and the manuscript provide the means to deal with two of these (downscaling and parametric). However, the major or core issue identified by reviewer #2, structural uncertainties introduced by unquantified/unknown processes, remains a challenge for the scientific discipline to tackle and is far beyond the scope of this paper.

Unlike in physics, in palaeo-ice sheet modelling and other Earth Sciences the relationship between data and theory is not straightforward. This complex relationship is exemplified in continental drift, which was proposed in the 1920s but only confirmed by data in the 1960s. For palaeo-ice sheet modelling, there are comparable uncertainties in both the models and the data, and comparison is required for the science to evolve and move forward. ATAT is a step forward for palaeo-ice sheet modelling; it adopts a set of repeatable procedures to compare data and model outputs and permits users and the communities to draw conclusions on how to progress. The procedures in ATAT and discussed in the manuscript account for model-based and data-based uncertainty. However, structural uncertainties introduced by as yet unknown theoretical advances and/or advances in data cannot be accounted for.

We have addressed the concerns of reviewer #1 by adding additional documentation and an example ice grid.

Thank you again for your consideration of this manuscript.

Reviewer #1

I'd like to thank the authors for addressing the comments by myself and Dr. Tarasov. I think the text is in good shape, I have a couple of minor comments below. However, I still think that the documentation of the program is a bit lacking to easily use it. The authors have now included a sample dates file, but did not give an example ice thickness/mask file that would give a template of how to design the NetCDF file. I tried to get some files together myself to run it, but I gave up after a few hours. As an example of my confusion, Table 3 in the text states the dimensions are [x,y], however the program expects coordinates of [x1,y1]. Maybe the program could have the option to detect which coordinates are in the given NetCDF file?

Thank you for these two thorough and constructive reviews. We have added some text with the aim of helping the reader develop input grids to the general instructions section of the manuscript (lines 602-612), and provided an example ice thickness grid. We have also made updated the reference data to have the more standard coordinate names x and y.

Minor comments in the text:

Line 52: Maybe explicitly name these two tools.

The two tools are now named in the text.

Figure 8: I still think it is extremely hard to make out anything from the age data points in this figure, it looks like a bunch of tiny red dots. Although I am aware that you are using a high resolution, and you want to show the data at the resolution of the study area, but I still think it would look a lot better to show the data points at a size that the ages can be discerned.

The size of the points on Figure 8 have now been increased.

Reviewer #2

Though the revised submission and software is an improvement, there remains a core problem. As detailed below, there is a fundamental contradiction in the paper that needs to be addressed. The authors rigorously defend their inclusion of discussion on model and data uncertainties but then ignore these uncertainties in their metrics. For model calibration in the context inferring past ice sheet evolution, a metric needs to take into account all uncertainties, otherwise the resulting inferences will be invalid. And even for the context of just data/reconstruction comparison, inferential uncertainties (measurement, dating, downscaling) need to be accounted for. The two RMSE metrics (equations 1 and 2) could easily be modified to account for observational and downscaling uncertainties.

Our responses to reviewer #2 assume the following three categories of model-based uncertainty: (i) downscaling uncertainty – caused by changes in grid resolution when comparing between models and data; (ii) parametric uncertainty – a consequence of uncertain parameters and boundary conditions input into the model; and (iii) structural uncertainty – that which is introduced into a model by a lack of physical understanding of a system (in this

case an ice sheet). We define this here, and in the manuscript (lines 191 onward) to avoid confusion over nomenclature.

The previous iteration of reviews addressed downscaling uncertainty by altering the ATAT code. Parametric uncertainty is often addressed in ice-sheet modelling by conducting ensemble experiments. ATAT can then be used to rule out simulations which perform particularly badly against the data, choose simulations which perform well and quantify the misfit between a single model run and the data. Our means of accounting for parameter uncertainty is therefore to assume that an ensemble of experiments has been conducted, and that ATAT is used to quantify how each individual performs at replicating the timing of ice-free conditions in the geochronological data. Therefore, the handling of parameter uncertainty is left to the user, who should account for this when designing model experiments. This rationale is stated and developed in lines 82-88, 288-295, 473-489, and 568-572.

Since structural uncertainty encompasses all the processes that are poorly understood or unknown to science, a degree structural uncertainty will always remain (unless in the extreme case a system is fully understood, in which case the scientists involved can move onto a different discipline). It is unclear how one would quantify the effects of processes unknown to science within a model. Therefore, that such structural uncertainties exist should be a caveat of any modelling paper, as well as a justification for a scientific discipline to continue to be curious about how a system operates. In the case of ice sheet modelling, it is also unclear how such structural uncertainties caused by unknown processes could be expressed in years, and therefore be comparable to the geochronological data.

Our pragmatic approach would be to compare multiple model outputs, which combined cover plausible ranges of parameters and known processes, to the data, in the way described in ATAT. This may ultimately reveal model-data misfits which mean that structural uncertainties need to be resolved (i.e. we need to better understand this process to fit this data). For example, one could envisage a modelling experiment which included two models, one which does not include a newly implemented process and one which does. Assuming all other things are left equal, ATAT could be used to quantify how introducing an additional process into the model may influence the degree of fit to the model (this idea is also now included in the manuscript (lines 484-489)).

Inferential (data/reconstruction-based) uncertainties are accounted for by ATAT. As listed at the bottom of Figure 5, numerous metrics are calculated by ATAT. Data and model-based uncertainties are included in these metrics. The paper details how it is determined whether a dated site agrees with a model simulation or not (Figures 3 and 5, lines 423-433). This comparison considers the error associated with a dated site and in the latest iteration, elevation and margin uncertainties in the model. This categorises dates as to their accordance with the model output in question and produces a “Percentage of dates within error with margin uncertainty metric.” We then apply the RMSE metrics to only those sites that agree within dating error, modelled margin and modelled elevation uncertainty. In this way, our metrics consider dating and model uncertainty. This is described in lines 456-467, a section we have extended and amended to address the concerns of reviewer #2. Other metrics are also retained, so that users may utilise less stringent metrics. We expect these to be useful in cases where no agreement between data and a model occurs when all uncertainties are considered. A user may then want to distinguish between model runs which get close to

matching data, and those that are then far away from the data. This additional point is now included in the manuscript on lines 465-467.

The user also needs to be provided with clear simple instructions for modifying the metric to do so to insert their own estimates for structural uncertainty. Without these corrections, I suspect ATAT will foster invalid model/data based inferences and thereby do a disservice to the community.

As noted in the previous response, ATAT assumes that a model has been run multiple times in an ensemble experiment or sensitivity analysis, as occurs frequently in ice sheet modelling (and as is noted in lines 15, 17, 78, 84, 179, 223, 293, 299, 328, 470, 475, 501, 576). Perturbing inputs over a range of plausible values, such ensembles are designed to account, at least partially, for the parametric uncertainty in input parameters for processes implemented in the model. As demonstrated above, this is stated throughout the manuscript, but perhaps most pertinently at lines 178-180, 293-295 and 328-329.

ATAT could also be used on the amalgamation of an ensemble experiment. For example, if a grid showing the mean deglacial age from an ensemble was produced, ATAT could be used to identify how well this mean replicates the data points. One could also envisage considering the uncertainty associated with this modelled age (e.g. a standard deviation of simulations) when producing a modelled uncertainty grid. This and other potential pragmatic uses are now explicitly stated in lines 473-489. Despite these suggestions, the role of this paper is to describe and provide a tool, not an experimental design.

How to account for structural uncertainty, which is essentially unknown until ice sheets are better understood and more (as yet unknown/unquantified) processes incorporated into models, is unclear. Reduction of this uncertainty remains a challenge for the discipline (line 232).

detailed comments : responses and revised text

“In reality, with a high-resolution ice-sheet model (say 5 km) it is unlikely that two equally reliable dates will be contained within a cell – radiocarbon in a core for example should just use the date that is oldest, closest to the glacial contact.”

The expense of 5 km resolution paleo ice sheet models precludes their current useage for the large ensembles needed for paleomodel calibration. Also, in regions with high-topographic variance (eg most of the Greenland margin), there may easily be two relevantly valid dates within 5 km proximity at different elevations.

We accept that there may be two dates within a cell, and have added the caveat that since we are testing deglaciation, the date considered to be most representative of final deglaciation of a cell should be considered (lines 367-371).

“Tarasov et al. 2012 run ice sheet models that are not independent of the dated chronology (there is a margin raster, their Fig 2, which “nudges” the ice sheet into place based upon Dykes reconstruction).” # Not clear what you mean by "independent", the margin chronology (with uncertainties) is used for nudging the surface mass-balance within climate

forcing uncertainties (nudging isn't unbounded), but the amount of nudging then goes into the cost function for the calibration.

This is a misunderstanding on our part, our apologies to reviewer #2.

>If this tool is meant to be used by those doing model calibration against paleo observations, then model uncertainty and downscaling error needs to be explicitly accounted for in the metric.

“We have shortened the length of this discussion, but retain the section as we think that understanding the uncertainty of the model is important when comparing to data. Uncertainty handling will come with ensemble design, the tool asks which ensemble member fits the data best.”

The authors never respond to my concern above about model uncertainty (ie structural uncertainty). They thereby also contradict their own stated requirement in the text: "In order to maximise the benefit to all users, any comparisons between palaeo-ice sheet model output and empirical data should ideally consider the inherent uncertainties of both."

As detailed above, ATAT does consider both data (measurement, reconstruction) and model uncertainty. We consider data uncertainty in the agree/disagree criteria (lines 456-458). Downscaling uncertainty is considered in the elevation and margin uncertainty calculation, added in the previous iteration of review. Parametric uncertainty should be considered in experimental design, as we frequently note throughout the manuscript. Structural uncertainty will always exist to some extent, but is difficult to quantify as noted in our responses above.

Furthermore, if the user of ATAT is going to rely on either the original or current descriptions of dating and modelling uncertainty as their main source of understanding these critical issues, then the paper will be doing a disservice to the community. The main message should be that users need to invest the time to really understand these uncertainties or include a collaborator who does.

The provision of a set of in depth appropriate references on this topic would therefore be of much more use than the current or past version cursory discussions.

We have reiterated that readers should look elsewhere for further understanding of data and modelling issues, and that this is a necessary overview before describing a tool, not a review paper (lines 96-99). This background section has numerous references to relative issues, made shorter on the request of the reviewers in the previous round of reviews. We have also added that collaboration between relevant parties is key (lines 99-101).

“Uncertainty handling will come with ensemble design, the tool asks which ensemble member fits the data best.”

The first phrase is incorrect and the 2nd means the tool is useless for model calibration in the context of inferring past ice sheet evolution. Read Rougier, 2007 to understand what structural uncertainty means and why it has to be included in the likelihood function. The 2nd phrase what are the comparative fits of each ensemble member to the constraint data given all uncertainties.

As stated above, we show that one can use ATAT whilst model-based uncertainty by conducting an ensemble (we have know of no other practical means exists of handling parametric uncertainty). Acknowledgement to Rougier (2007) has been made to point the reader to a more detailed discussion of model uncertainty in general (lines 98 and 190). We note though that this paper deals with meteorological model-data comparison. Although some parallels can be drawn to ice sheet model-data comparison, the data has completely different qualitative and quantitative characteristics, and therefore does not solve the problem of comparing ice sheet models with data.

We reiterate, this is a paper which describes a tool and ways in which it may be useful. This tool and the statements in the paper consider data-based and model uncertainties.

“It is also important keep the agree/disagree metric for the following reason: you may do 100 simulations of a palaeo ice sheet and keep getting the same sites that disagree.”

I don't follow the logic here. What does agree/disagree mean? Your responses seem to put a lot of emphasis on user choice, but here you are imposing a choice on what level of misfit constitutes disagreement instead of having the user apply their "expert judgement"...

Lines 425-433 describe what we mean by agree/disagree, whether a model and data point both agree on ice-free timing. There is also a figure on this (Figure 3) and a worked example of how ATAT identifies where model-data agreement/disagreement occurs (Figure 9A). We do not impose a choice on what constitutes misfit, we leave this to the user as they can define the level of data error in the input files. This is described in lines 376-379.

“Three classes of data are of particular use for constraining palaeo-ice sheets; 46 (i) geomorphological data, (ii) relative sea level history, and (iii) geochronological data”

This list is too limited. Present-day rates of vertical uplift are also a powerful constraint (cf my 2012 paper) for the North American and Eurasian ice sheets. So change RSL -> geophysical constraints (including RSL and present-day vertical velocities).

This has been amended in the text accordingly (lines 47 and 56-59).

“applying offsets derived from ice core records to contemporary climate (Hubbard et al., 2009) and scaling 202 between present-day conditions and uncoupled global-circulation-model simulations at maximum glacial 203 conditions (Gregoire et al., 2012; Gasson et al., 2016).”

The usual standard for example references is either a recent detailed review or first use. The above citations do not follow either logic.

In the absence of a review of palaeo-ice sheet modelling climate forcing techniques, we have added additional reference to early use of the methods.

“Since all dating 390 techniques only record the absence of ice, geochronological data provides only a one-way constraint on palaeo-391 ice sheet activity. For deglacial ages, deglaciation could occur any time before the geochronological data provided 392 and within the error of the date,”

Incorrect. As detailed:

We are unsure how this is incorrect, as we are describing how all deglacial (advance) dates are minimum (maximum) constraints (see below).

Figure 3

I am concerned about the metric indicated in this figure. It seems to indicate that a model with say last retreat for a given grid cell at say 30 ka, will be given the same score for this site as for a model that retreats ice at say 19 ka (for the given sample date of 18 +/- 1 ka). If my interpretation is correct, this needs to be remedied. This should be obvious for eg cosmogenic dates where inheritance will make the date if anything too old (and therefore cosmogenic dates may be maximum limiting depending on type of sample and location). But even for C14 dates, where the issues of sample availability, time required for in-migration of plants,.. mean that the dates are generally minimum limiting, I can't see anyone saying that a model with a 12 kyr misfit with a minimum limiting age should score the same as a model that fits the sample within sample age uncertainties.

Firstly, this is a schematic for deriving whether an age agrees or disagrees with a model, whilst accounting for error of the age, not a metric in itself. Closeness of fit is assessed later. Clarification of this has been made in the figure caption. Secondly, the statement that the example given would provide the same score is incorrect. The 30ka retreat would be identified as model-data agreement (strictly this is acceptable given that all deglacial ages are treated as minimum constraints) but the RMSE scores would be heavily effected by a difference of 12ka, and this outlier will be evident on the produced model-data offset map (e.g. Figure 9B). We are aware of the issue and it is already described in the manuscript (lines 309-317) with the suggestion that loose constraints are removed from comparison data by initial data filtering (lines 372-374). Thirdly, cosmogenic dates can be considered as minimum limiting. There are processes that make a cosmogenic date too young, for example vegetation/sediment cover and post glacial depositional erosion. Erosion specifically is more likely to affect all samples from a site to a broadly similar degree and the erosion rate must be assumed in calculating an exposure age. Erosion rates are generally assumed to be low (e.g. 0 -1 mm ka⁻¹) but higher rates (for whatever reason) would cause the apparent exposure age to be too young. While inheritance can be an issue, it is common practise for multiple samples to be considered in cosmogenic dating and ages that clearly exhibit inheritance can be excluded (the reference of Small et al. 2017 which we repeatedly refer to details this further). Conversely, unquantified error introduced by an incorrect assumption of erosion rate would potentially affect all ages from a site to a broadly similar degree and thus said ages may not warrant exclusion.

equations 1 and 2 are highly problematic given that observational and model uncertainties are ignored. And this again contradicts the authors own statements about the importance of these uncertainties.

Observational uncertainties are not ignored in the calculation of these metrics, as they are applied to categories of data according to whether model-data agreement occurs when considering the associated error of an age (this is now more explicitly stated in lines 462-467. and on Figure 5). Downscaling (margin and vertical) uncertainties of the model are now accounted for in ATAT (due to previous reviews, stated on lines 410-421). Parametric uncertainties can be overcome to some extent by ensemble experiments, and this is stated in the text (see previous responses and lines 475-478).

ATAT 1.1, an Automated Timing Accordance Tool for comparing ice-sheet model output with geochronological data

Jeremy C. Ely¹, Chris D. Clark¹, David Small² and Richard C.A. Hindmarsh³

¹Department of Geography, The University of Sheffield, Sheffield, S10 2TN, UK

²Department of Geography, Durham University, Durham, DH1 3LE, UK

³British Antarctic Survey, High Cross, Madingley Road, Cambridge, CB3 0ET, UK

Correspondence to: Jeremy C. Ely (j.ely@sheffield.ac.uk)

Abstract. Earth's extant ice sheets are of great societal importance given their ongoing and potential future contributions to sea-level rise. Numerical models of ice sheets are designed to simulate ice sheet behaviour in response to climate changes, but to be improved require validation against observations. The direct observational record of extant ice sheets is limited to a few recent decades, but there is a large and growing body of geochronological evidence spanning millennia constraining the behaviour of palaeo-ice sheets. Hindcasts can be used to improve model formulations and study interactions between ice sheets, the climate system and landscape. However, ice-sheet modelling results have inherent quantitative errors stemming from parameter uncertainty and their internal dynamics, leading many modellers to perform ensemble simulations, while uncertainty in geochronological evidence necessitates expert interpretation. Quantitative tools are essential to examine which members of an ice-sheet model ensemble best fit the constraints provided by geochronological data. We present an Automated Timing Accordance Tool (ATAT version 1.1) used to quantify differences between model results and geochronological-data on the timing of ice sheet advance and/or retreat. To demonstrate its utility, we perform three simplified ice-sheet modelling experiments of the former British-Irish Ice Sheet. These illustrate how ATAT can be used to quantify model performance, either by using the discrete locations where the data originated together with dating constraints or by comparing model outputs with empirically-derived reconstructions that have used these data along with wider expert knowledge. The ATAT code is made available and can be used by ice-sheet modellers to quantify the goodness of fit of hindcasts. ATAT may also be useful for highlighting data inconsistent with glaciological principles or reconstructions that cannot be replicated by an ice sheet model.

1 Introduction

Numerical models have been developed which simulate ice sheets under a given climate forcing (e.g. Greve, 1995; Rutt et al., 2009; Pollard and DeConto, 2009; Winkelmann et al., 2011; Gudmundsson et al., 2012; Cornford et al., 2013; Pattyn, 2017). When driven by future climate scenarios, these models are used to forecast the fate of the Antarctic and Greenland ice sheets (e.g. Seddik et al., 2012; DeConto and Pollard, 2016), providing predictions of their potential contribution to future sea level rise. However, incomplete knowledge of ice physics, boundary conditions (e.g. basal topography) and parameterisations of physical processes (e.g. basal sliding, calving), as well as the difficulty of predicting future climate, lead to model-based (~~structural~~)-uncertainty in these predictions (Applegate et al., 2012; Briggs et al., 2014; Ritz et al., 2015). Observations of ice marginal fluctuations (decades) and the processes of ice calving, flow or melting (subaerial or submarine) that facilitate or drive such variations, provide a powerful means to understand the processes leading to the possibility of deriving new formulations that

37 improve the realism of modelling. However, the short-time span (decades) of these observations limits their being
38 used to constrain, initialise or validate modelling experiments (Bamber and Aspinall, 2013). Conversely, palaeo-
39 ice sheets, especially from the last glaciation (~21,000 years ago), left behind evidence which provides the
40 opportunity to study ice sheet variations across timescales of centuries to millennia, albeit with increased
41 uncertainty in exact timing.

42 Numerous modelling studies have aimed to simulate the growth and decay of palaeo-ice sheets, producing
43 hindcasts of ice-sheet behaviour (e.g. Boulton and Hagdorn, 2006; Hubbard et al., 2009; Tarasov et al., 2012;
44 Gasson et al., 2016; Patton et al., 2016). Results from these hindcasts may be compared with empirical data
45 recording ice sheet activity, so as to discern which parameter combinations produce results that best replicate the
46 evidence of palaeo-ice sheet activity. Three classes of data are of particular use for constraining palaeo-ice sheets;
47 (i) geomorphological data, (ii) ~~relative sea level history~~ geophysical data, and (iii) geochronological data. Ideally,
48 all three classes of data should be used to quantify the goodness of fit of a hindcast.

49 Geomorphological evidence comprises the landforms created by the action of ice upon the landscape, and can
50 typically provide data on ice extent, recorded by moraines and other ice marginal landforms and on ice-flow
51 directions recorded by subglacial landforms such as drumlins. Such landforms can be used to decipher the pattern
52 of glaciation (e.g. Kleman et al., 2006; Clark et al., 2012; Hughes et al., 2014). Two tools, namely Automated
53 Proximity and Conformity Analysis (APCA) and Automated Flow Direction Analysis (AFDA), have already been
54 developed which can compare modelled ice margins (APCA) and flow directions (AFDA) to the
55 geomorphological evidence base (Napieralski et al., 2007).

56 Geophysical data, in the form of rRelative sea level measurements and present day uplift rates, data provides
57 information regarding the mass-loading history of an ice sheet. Palaeo-ice-sheet model output is often evaluated
58 against ~~relative sea levels~~ such data by use of glacio-isostatic adjustment models (e.g. Tushingham and Peltier,
59 1992; Simpson et al., 2009; Tarasov et al., 2012; Auriac et al., 2016).

60 Geochronological evidence attempts to ascertain the absolute timing of ice advance and retreat using dated
61 material (e.g. organic remains dated by radiocarbon measurement) found in sedimentary contexts interpreted as
62 indicating ice presence or absence nearby. It enables reconstruction of the chronology of palaeo-ice sheet growth
63 and decay (Small et al., 2017) and is the underpinning basis for empirically-based ice sheet margin reconstructions
64 (e.g. Dyke, 2004; Clark et al., 2012; Hughes et al., 2016). Although widely used in empirical reconstruction of
65 palaeo-ice sheets, geochronological data has rarely been directly compared with ice sheet model output (although
66 see Briggs and Tarasov, 2013). Such a comparison could be useful both for constraining ice-sheet model
67 uncertainty and for identifying problems with the geochronological record. For example, a poor fit between model
68 output and empirical data on timing could inform on the validity of a numerical model (or its parameterisation),
69 or it could provide a physical basis for questioning the plausibility of empirically-driven interpretations or specific
70 lines/data points of evidence given that they are associated with inherent uncertainties. In order to maximise the
71 benefit to all users, any comparisons between palaeo-ice sheet model output and empirical data should ideally
72 consider the inherent uncertainties of both.

73 Given the wide availability of compilations of geochronological data (e.g. Dyke, 2004; Hughes et al., 2011;
74 Hughes et al., 2016), as well as the proliferation of ice sheet models (e.g. Greve, 1995; Rutt et al., 2009; Pollard
75 and DeConto, 2009; Winkelmann et al., 2011; Gudmundsson et al., 2012; Cornford et al., 2013; Pattyn, 2017), a
76 convenient, reproducible and consistent procedure for comparison should be of great utility to the palaeo-ice sheet

77 community. The typical volume of geochronological constraints (several thousands) for a palaeo ice sheet and the
78 number of ensemble runs (several hundreds) from an ice sheet model make a visual matching of data and model
79 output nearly impossible to accomplish, which is likely to explain the rarity of such comparisons. Here, we present
80 an Automated Timing Accordance Tool (ATAT, version 1.1). ATAT a systematic means for comparing ice-sheet
81 model output with geochronological data, which quantifies the degree of fit between the two. To separate model
82 uncertainty from data error, a single run of ATAT focuses on the error in geochronological data. This is achieved
83 by comparing geochronological data and its associated error to predictions of ice cover from single ice sheet model
84 output. However, through multiple comparisons against all members from an ensemble ice-sheet modelling
85 experiment, model parameter uncertainty can be considered by assessing the degree of fit to the various input
86 parameter combinations, an ice sheet model ensemble which considers model uncertainty, Therefore, ATAT could
87 be used as a basis for examining whether model-data mismatch is a consequence of inadequacies in either the
88 model or data. The tool is in the form of a Python script and requires the installation of open-source libraries.
89 ATAT is written to handle NETCDF data as an input, a format commonly used in ice sheet modelling and is also
90 accessible from many GIS packages in which geochronological data can be stored and manipulated.

91 **2 Background**

92 Geochronological evidence and ice sheet model outputs are often independently used to reconstruct the timing of
93 glaciological events. The two approaches are fundamentally different in nature and consequently produce
94 contrasting data outputs. Thus, before describing our approach to comparing the two sets of data (ATAT), we first
95 briefly consider the nature of both geochronological data and ice-sheet model output to highlight the issues and
96 potential difficulties associated with comparing the two and conceptualise a comparison procedure. More
97 extensive descriptions of the nature, uncertainties and limitations of glacial geochronological (Hughes et al., 2016;
98 Small et al., 2017) and model-based (Rougier, 2007; Tarasov et al., 2012; Briggs and Tarasov, 2013) data are
99 considered elsewhere. Given the complex nature of both, those seeking to compare geochronological data and
100 ice-sheet model output should ideally collaborate with those who understand the limitations and uncertainties
101 involved with both forms of data.

102 **2.1 Geochronological data**

103 The timing of palaeo-ice sheet activity has primarily been dated using three techniques: (i) radiocarbon dating;
104 (ii) cosmogenic nuclide exposure dating, and (iii) luminescence dating (Figure 1). The utility of each method for
105 determining the timing of palaeo-ice sheet activity has been extensively reviewed elsewhere (e.g. Fuchs and
106 Owen, 2008; Balco, 2011; Small et al., 2017) and only a brief description is provided here. Radiocarbon dating
107 uses the known rate of the radioactive decay of ^{14}C to determine the time elapsed since the death of organic
108 material (Libby et al., 1949; Arnold and Libby, 1951; Figure 1). For palaeo-glaciological purposes, the dated
109 organic material (e.g. shells, mosses, plant remains) is usually taken from basal sediments overlying and closely
110 associated with a glacial deposit in order to determine a minimum deglaciation age (e.g. Heroy and Anderson,
111 2007; Lowell et al., 2009); ice is interpreted to have retreated from this site some short time prior to this age.
112 Where organic matter is either reworked within or is located directly beneath a glacial deposit, it can be used to
113 constrain the maximum age of glacial advance (e.g. Brown et al., 2007; Ó Cofaigh and Evans, 2007); advance

114 happened sometime after this age. Cosmogenic nuclides (e.g. ^{10}Be , ^{26}Al and, ^{36}Cl) are produced by the
115 interaction of secondary cosmic radiation in minerals, such as quartz, within materials exposed at the Earth's
116 surface (Figure 1). Samples are generally taken from glacially-transported boulders, morainic boulders and
117 glacially modified bedrock, all of which have ideally had signals from any previous exposure history removed by
118 glacial erosion. Cosmogenic nuclide dating is thus used to determine the duration of time a sample has been
119 exposed at the Earth's surface by determination of the concentration of cosmogenic nuclides within that sample.
120 Luminescence dating can determine the age of a deposit by measuring the charge accumulated within minerals.
121 This charge accumulates in light-sensitive traps within the crystal lattice due to ionizing radiation produced by
122 naturally occurring radioactive elements (e.g. U, Th, K). Luminescence dating determines the time elapsed since
123 the last exposure of the mineral to sunlight; this exposure acts to reset the signal (Figure 1). As subglacial deposits
124 are unlikely to have been exposed to light before burial, and therefore contain signals accumulated prior to
125 deposition, luminescence dating within palaeo-glaciology is typically applied to ice marginal sediments, or those
126 which overly glacial sediments (e.g. Duller, 2006; Smedley et al., 2016; Bateman et al., 2018). All
127 geochronological techniques record the absence of grounded ice. They therefore provide either maximum or
128 minimum ages of a glaciological event, depending upon the stratigraphic setting. Table 1 outlines a commonly
129 used system used to classify geochronological data by stratigraphic setting (Hughes et al., 2011; 2016).
130 The retreat/advance (ice-free) ages provided by the three geochronometric techniques are all affected by
131 systematic and geological uncertainties (Small et al., 2017). Systematic uncertainties originate from the tools and
132 techniques used to derive the date, such as laboratory instruments and sample preparation, and are accounted for
133 in the quoted errors that accompany a date. Geological uncertainties are caused by the geological history of a
134 sample, before, during and after a glacial event (e.g. Lowe and Walker, 2000; Lukas et al., 2007; Heyman et al.,
135 2011). Such influences may leave little or no evidence of their effect upon a sample and are thus hard to quantify.
136 The relationship between a dated sample and the glacial event it indicates is the largest potential source of
137 uncertainty in geochronological data and is primarily bounded by the ability of the investigator to find and
138 associate dateable material to the glacial event of interest. Since all geochronological techniques measure the
139 absence of ice, expert inference must be made, and are influenced by the availability of information (stratigraphic
140 or otherwise) at a study site; they may be open to change (e.g. new radiocarbon calibrations, new cosmogenic
141 isotope production rates). Furthermore, in the cases of luminescence and radiocarbon dating, there can be an
142 unknown duration since glacial occupation of an area and the deposition of dateable material. These factors mean
143 it is necessary to consider the quality of dates for ascertaining the timing of the glacial event in question (Small et
144 al., 2017).
145 Numerous geochronological studies have sought to ascertain the timing of palaeo-ice sheet activity at sites, leading
146 to compilations of geochronological data which bring together hundreds to thousands of published dates (e.g.
147 Dyke et al., 2002; Livingstone et al., 2012; Hughes et al., 2011; 2016). Despite the growing number of reported
148 dates, they are still insufficient in number and spatial spread to define, on their own, the time-space envelope of
149 the shrinking ice sheet. Techniques to interpolate geochronological information between sites are required. The
150 most commonly used technique is empirical ice sheet reconstruction (e.g. Dyke, 2004; Clark et al., 2012), whereby
151 expert assessments of the geochronological and geomorphological record are used together to create ice-sheet
152 wide isochrones of ice-sheet margin position and flow configuration. A recent advance in this method has been
153 the inclusion of confidence envelopes for each isochrone, documenting possible maximum, likely and minimum

154 extents (Hughes et al., 2016). Further techniques for spatiotemporally interpolating geochronological data include
155 Bayesian sequence modelling (e.g. Chiverrell et al., 2013; Smedley et al., 2017), in which collections of deglacial
156 ages are arranged in spatial order determined by a priori knowledge of geomorphologically-informed ice flow and
157 retreat patterns (e.g. Gowan, 2013). Such techniques provide viable methods for producing ice-sheet wide
158 chronologies, filling in information in locations where geochronological data may be sparse.

159 **2.2 Ice sheet model output**

160 Ice-sheet models solve equations for ice flow over a computational domain, for a given set of input parameters
161 and boundary conditions, to determine the likely flow geometry and extent of an ice sheet. Typically, ice-sheet
162 models run using finite difference techniques on regular grids (e.g. Rutt et al., 2009; Winkelmann et al., 2011).
163 Ice-sheet models that utilise adaptive meshes (e.g. Cornford et al., 2013) and unstructured meshes also exist (e.g.
164 Larour et al., 2012) and the results from such models can be interpolated onto spatially regular grids. The spatial
165 resolution of an ice-sheet model depends upon the computational resources available, and the spatial resolution
166 of available boundary conditions. Continental-scale models of palaeo-ice sheets have typical spatial resolution of
167 tens of kilometres (e.g. Briggs and Tarasov, 2013; DeConto and Pollard, 2016; Patton et al., 2016), though parallel,
168 high-performance computing means higher resolutions are possible (e.g. 5 km in Golledge et al., 2013 and
169 Seguinot et al., 2016). The temporal resolution of ice sheet model output is ultimately limited by the time-steps
170 imposed by the stability properties of the numerical schemes solving the ice-flow equations. Given that these
171 stable time-steps can be sub-annual, output frequency is mostly predetermined by the user (typically decades to
172 centuries), and as such is constrained by available disk-storage. Ice-sheet models therefore produce spatially
173 connected predictions of ice-sheet behaviour such as advance and deglaciation (e.g. Table 1) across gridded
174 domains at various temporal and spatial resolutions.

175 The stress fields imposed upon ice can be fully described by solving the Stokes equations. Indeed, ‘full Stokes’
176 models which do so have been tested (Pattyn et al., 2008) and used to simulate ice sheets (e.g. Seddik et al., 2012).
177 However, fully solving the Stokes equations over the spatio-temporal scales relevant to palaeo-ice sheet
178 researchers remains beyond the limit of currently available computational power. This problem is exacerbated by
179 the need to run multi-parameter valued ensemble simulations to account for model uncertainty over multi-
180 millennial and continental-scale domains. This means that palaeo-ice sheet modelling experiments rely upon
181 approximations of the Stokes equations (see Kirchner et al., 2011 for a discussion), such as the shallow ice
182 approximation (SIA) and shallow shelf approximation (SSA). The choice of ice-flow approximation used within
183 a model has implications for the capability of models to realistically capture aspects of ice sheet flow (Hindmarsh,
184 2009; Kirchner et al., 2011; 2016), and in turn influences the nature of the model output produced. For instance,
185 the SIA is not applicable for ice shelves, therefore SIA-based models do not produce modelled ice shelves (e.g.
186 Glimmer; Rutt et al., 2009). Therefore, the timing of deglaciation in an SIA model can be determined as the point
187 at which ice thickness in a cell becomes zero or thinner than the flotation thickness, whereas in a SSA or higher-
188 order model the location and movement of the grounding line must be determined.

189 Though ice sheet models produce output which is consistent with model physics, [like all numerical models of](#)
190 [physical systems \(e.g. Rougier, 2007\)](#) there are many sources of uncertainty involved with ice sheet modelling.
191 [Three broad sources of model-based uncertainty can be distinguished: \(i\) down-scaling; \(ii\) parametric](#)
192 [uncertainty; \(iii\) structural uncertainty. These are defined and discussed below.](#)

193 [Down-scaling uncertainties arise due to an ice-sheet models computation over space which has a coarser resolution](#)
194 [than reality. This means that a characteristic which can be measured to a high level of accuracy and precision for](#)
195 [a real ice-sheet \(e.g. the position of a calving front\), has a larger uncertainty in an ice-sheet model. This is](#)
196 [especially pertinent for data-model comparisons, as most observations of ice-sheet activity have a sub-model](#)
197 [resolution.](#)

198 ~~Parametric~~[This model-based \(structural\)](#) uncertainty has two main sources: (i) parameterisations, and (ii)
199 boundary conditions. Where a process is too complex (e.g. calving) or occurs at too small a scale (e.g. regelation)
200 to be captured by an ice sheet model, it is often simplified and parameterised. Associated with each
201 parameterisation are a set of parameters, the values of which are either unknown, or thought to vary within some
202 plausible bounds, and which can either be constant or spatially and temporally variable across a domain. An
203 example of a process which is often parameterised is basal sliding. This parameterisation is often done through
204 the implementation of a sliding law (e.g. Fowler, 1986; Bueller and Brown, 2009; Schoof, 2010), which relates the
205 basal shear stress to the basal velocity (Fowler, 1986). Parameters used to determine this relationship are often
206 assigned or incorporated within a parameter, or prescribed by another model parameterisation (e.g. a subglacial
207 hydrology model). Adding to the uncertainty in the absence of a single preferable sliding law, ice-sheet models
208 often allow the user to choose between different sliding law implementations.

209 Boundary conditions, the values prescribed at the edge of the modelled domain, also introduce uncertainty into
210 ice-sheet models. For contemporary ice sheets, there is a large uncertainty in the basal topography (e.g. Fretwell
211 et al., 2013). This is less of a problem for the more accessible beds of palaeo-ice sheets. However, accurately
212 accounting for the evolution of this bed topography over the course of a glaciation requires a model of isostatic
213 adjustment (Lingle and Clark, 1985; Gomez et al., 2013).

214 A very large source of uncertainty for modelling palaeo-ice sheets is the climate used to drive them (Stokes et al.,
215 2015), as indeed is the case for forecasts of contemporary ice sheets (e.g. Edwards et al., 2014). Owing to the
216 computational resources required and technical challenges, few palaeo-ice sheet models are coupled with climate
217 models. This uncertainty over past climate is reflected in the large range of outputs produced by global circulation
218 models which have tried to simulate the last glacial cycle (e.g. Braconnot et al., 2012). Palaeo-ice sheet modellers
219 have used a range of methods to force their models, including simple parameterisations (Boulton and Hagdorn,
220 2006), applying offsets derived from ice core records to contemporary climate (e.g. Huybrechts, 1990; Hubbard
221 et al., 2009) and scaling between present-day conditions and uncoupled global-circulation-model simulations at
222 maximum glacial conditions (e.g. Greve et al., 1999; Gregoire et al., 2012; Gasson et al., 2016). Each approach is
223 associated with an inherent uncertainty. When this uncertainty is accounted for [in an ensemble experiment](#), the
224 range of possible climates produces numerous ice sheet outputs.

225 [Structural uncertainty is related to parametric uncertainty, but has a broader remit, and is defined here as all](#)
226 [uncertainty that arises within a model due to a lack of physical understanding of the system in question. In this](#)
227 [broad sense, structural uncertainty encompasses all processes which are not incorporated in a model. This may](#)
228 [include some processes which are well understood, but not included in a model due to the lack of a numerical](#)
229 [formulation, for computational efficiency, or because they are deemed unimportant for the question being studied.](#)
230 [In a broader sense, structural uncertainty also includes processes that are as yet unknown to science and therefore](#)
231 [are not implemented in a model. Reducing structural uncertainty, by including additional pertinent processes in](#)
232 [models, is an ongoing challenge for ice-sheet modelling.](#)

233 There is another [structural uncertainty cause of which hinders](#) ice-sheet models ~~not from~~ being able to accurately
234 predict the evolution of ice-sheets, which is the presence of instabilities – we use this term in the technical sense
235 of a small perturbation ~~that in-~~ leads to the whole ice-sheet system amplifying this small perturbation to the extent
236 it can leave a mark in the geological record. A classic example of this in ice-sheet dynamics is the marine ice-
237 sheet instability (MISI), first discussed in the 1970s (Hughes, 1973; Weertman, 1974, Mercer, 1978) and more
238 recently put on a sounder mathematical footing (Schoof 2007, 2012).

239 The MISI actually refers to an instability in grounding-line (GL) position on a reverse slope, where the water
240 depth is shallowing in the direction of ice flow. Since ice flux increases with ice thickness, a straightforward
241 argument leads to the conclusion that if the GL advances into shallower water, the efflux will decrease, the ice
242 sheet will gain mass and the advance continue. If, on the other hand, the GL retreats, the flux will increase, the
243 ice-sheet will lose mass and the retreat continue. In principle, given the right parameterisations and basal
244 topography, ice-sheet models should be able to predict the ‘trajectory’ of GL migration arising as a consequence
245 of the MISI. However, the MISI is one of the class of instabilities that lead to poor predictability; certain small
246 variations of parameters and specifications will lead to large-scale changes in the ‘trajectory’, in this case the
247 retreat history. A well-known analogy is the ‘butterfly effect’, which originated in atmospheric modelling work
248 (Lorenz, 1963); the butterfly effect is concerned with the consequences of the statement “small causes can have
249 larger effects”. Recent work has also shown that additional physical processes, such as ice-shelf buttressing
250 (Gudmunsson, 2012) and the effect that the gravitational pull of ice-sheets has on sea level (Gomez et al., 2012)
251 have additional effects on grounding line stability. Given that most of the palaeo-ice sheets during the last glacial
252 cycle had extensive marine margins and overdeepened basins, with isostatic adjustment creating further zones of
253 reverse slope, capturing grounding line processes is important for simulating these ice-sheets.

254 **2.3 Considerations when comparing geochronological data and ice-sheet model output**

255 Sections 2.1 and 2.2 make it clear that several factors must be considered in order to satisfactorily compare
256 geochronological data and ice-sheet model output (Table 2). Most critically, the two datasets involved in any
257 comparison have varying spatial properties. Raw geochronological data is unevenly distributed and located at
258 specific points, with horizontal position accurate to a metre or so; such data may be used to plot ice-margin
259 fluctuations of the order of tens of kilometres (Figure 2C). Ice-sheet models typically produce results on evenly-
260 spaced points (at ~5 km to 20 km resolution) that are distributed over and beyond the maximum area of the palaeo-
261 ice sheet (Table 2; Figure 2B). Consequently, in comparing the two, a choice must be made; either
262 geochronological data should be gridded (coarsened) to the resolution of the ice-sheet model, or the ice-sheet
263 model results must be interpolated to a higher resolution. Both options have drawbacks, as the former removes
264 spatial accuracy from geochronological data while the latter relies upon interpolation beyond model resolution
265 and, more seriously, model physics. A second problem lies in the spatial organisation of the data (Table 2). Ice-
266 sheet models produce a regular grid of data (Figure 2B), meaning that no location is more significant than any
267 other when comparing the modelled deglacial chronology with that inferred from geological data. Conversely,
268 owing to the uneven distribution of raw geochronological data, some regions of a palaeo-ice sheet may be better
269 constrained than others (Figure 2C). As noted by Briggs and Tarasov (2013), any comparison that does not treat
270 the uneven spatial distribution of geochronological data may favour sites where numerous dates exist over more
271 isolated locations. One approach to overcoming these disparities is to use an interpolation scheme (e.g. empirical

272 reconstruction, Bayesian sequence) on the raw geochronological data. This produces a geochronological
273 framework by combining evidence on pattern and timing to yield a distribution that is spatially more uniform and
274 a spatial resolution similar to that of palaeo-ice sheet model output (Figure 2D).

275 The temporal intervals between and precision of geochronological data and ice sheet model output also vary
276 (Table 2). The time intervals between geochronometric data are determined by the number of available
277 observations, and precision determined by sources of uncertainty. Conversely, ice sheet models produce output at
278 regular intervals and are temporally exact, which is to be contrasted with ‘correct’. Since the output interval of an
279 ice-sheet model is generally determined by the user (see Section 2.2) it is pertinent to consider an appropriate
280 time-interval of ice-sheet model output for comparison with geochronological data. For example, radiocarbon
281 dates have precision typically in the order of hundreds of years but do not directly constrain ice extent, whilst
282 empirically reconstructed isochrones are typically produced for thousand-year time-slices (e.g. Hughes et al.,
283 2016). In reality, ice-sheets may respond to events at faster time-scales than this, but in the absence of internal
284 instabilities (e.g. MISI) palaeo-ice sheet models are ultimately limited by the temporal resolution of the available
285 climate forcing data. Thus, to gain insight into controls on palaeo-ice sheet behaviour, it may be necessary to
286 create model output with a greater (centurial) temporal resolution than the uncertainty associated with
287 geochronology.

288 Both geochronological data and ice-sheet model output have sources of uncertainty which must also be considered
289 when comparing the two. For geochronological data, uncertainty is typically expressed as a standard deviation
290 from the reported age, and are therefore easy to consider when comparing to an ice sheet model. For ice-sheet
291 models, individual model runs do not currently express uncertainty, and it is only when multiple, ensemble, runs
292 which systematically vary parameters and boundary conditions are conducted that uncertainty in all output
293 variables can be expressed. Therefore, any comparison between geochronological data and model simulations
294 must either compare to all members of an ensemble experiment in turn, or against amalgamated output from an
295 ensemble which considers model uncertainty. Having said this, statistical techniques exist to derive probability
296 distribution functions for individual quantities (e.g. Ritz et al., 2015). Such ensemble runs typically comprise
297 hundreds to thousands of individual runs (Tarasov and Peltier, 2004; Robinson et al., 2011). Given the volume of
298 data this produces, one appealing application of a quantitative comparison between geochronological data and ice
299 sheet model output would be to act as a filter for scoring ice-sheet model runs and reducing predictive uncertainty
300 by only using the parameter combinations that were successful. However, if all possible parameters have been
301 modelled, (i.e. the full ‘phase-space’ of the model has been explored (cf. Briggs and Tarasov, 2013)), and very
302 few (or no) model runs conform to a certain set of geochronological data or an empirical reconstruction, this may
303 provide a basis to question aspects of the evidence (e.g. re-examining the stratigraphic context of a dated sample
304 site or questioning the basis of the reconstructed isochrone). Of course, a third possibility that both data and model
305 are incorrect cannot be excluded.

306 We therefore suggest that any comparison between ice-sheet model experiments and geochronological data should
307 consider:

- 308 i) That both ice-sheet models and geochronological data have inherent uncertainties;
- 309 ii) That geochronological data typically provide a constraint on just the absence of ice; such that ice must have
310 withdrawn from a site sometime (50 years? 500 years? 5000 years?) prior to the date (which can be any point
311 within the full range of the stated uncertainty). It is thus a limit in time and not a direct measure of glacial activity.

312 Figure 3 illustrates this for advance and retreat constraints. It is most often the case that dated material is taken
313 close to the stratigraphic boundary or landform representing ice presence, in which case a date might be considered
314 as a ‘tight constraint’ (e.g. the ice withdrew and very soon afterwards (50 years) marine fauna colonised the area
315 and deposited the shells used in dating). Sometimes however there may have been a large (centuries to millennia)
316 interval of time between the withdrawal and the age of the shell chosen as a sample, in which case the date will
317 provide a ‘loose’ limiting constraint; it might be much younger than ice retreat (Figure 3).

318 iii) There is inherent value to the expert interpretation of stratigraphic and geomorphological information, meaning
319 an ice-free age reported for a site is likely as close as possible (tight constraint) to a glacial event. However, this
320 interpretation could be subject to change;

321 iv) Geochronological data exist as spatially distributed dated sites (e.g. Figure 2C) which can be built into a
322 spatially coherent reconstruction (e.g. Figure 2D);

323 v) A great input uncertainty in a palaeo-ice sheet model is the climate, which can lead to changes in the spatial
324 extent and timing of ice sheet activity.

325 vi) A factor which requires further investigation is the relationship between the operation of a physical instability
326 (e.g. the MISI) and the practical ability of models to predict retreat or advance rates; the presence of an instability
327 can result in extreme sensitivity to parameter ignorance or over-simplified model physics.

328 vii) Other uncertainties can also lead to variations in ice-sheet model results; these can be accounted for in an
329 ensemble of hundreds to thousands of simulations.

330 Given the above, it is unlikely that a single procedure could capture model-data conformity. ATAT therefore
331 implements several ways of measuring data-model discrepancies and produces output maps (described in the
332 following two sections) to help a user assess which model runs best agree with the available geochronological
333 data. One approach is to transform the geochronological data points (x,y,t) to a gridded field (raster) that define
334 age constraints of ice advance and another grid for retreat. Both of these data types also require an associated grid
335 that reports the uncertainty range as error (Figure 4). These age grids may then be quantitatively compared to
336 equivalent grids (age of advance grid and age of retreat grid) derived from the ice sheet model outputs.
337 Alternatively, one might prefer to compare model runs against the geochronological data (points) combined with
338 expert-sourced interpretive geomorphological and geological data, in which age constraints from dated sites have
339 been spatially extrapolated using moraines and the wider retreat pattern. In this case ATAT allows the model
340 outputs to be compared to the ‘lines on maps’ type of reconstruction subsequent to conversion from age isolines
341 to a grid of ages (Figure 4).

342 **3. Description of tool**

343 ATAT is written in Python, and utilises several freely available modules. Access to these modules may require a
344 Python package manager, such as ‘pip’ or ‘anaconda’. ATAT can therefore be run from the command line on any
345 operating system, or by using a Python interface such as IDLE.

346 **3.1 Required data and processing**

347 ATAT requires two datasets as an input: (i) an ice-sheet model output; and (ii) gridded geochronological data.
348 Table 3 provides the required variables and standard names for each dataset. In order to determine the advance

349 age or deglacial age predicted by the ice sheet model, ATAT requires either an ice thickness (where the model
350 does not produce ice shelves) or a grounded ice-mask variable (where ice shelves are modelled). In the latter case,
351 the user is asked to define the value which represents grounded ice.

352 Empirical advance and deglacial geochronological data (Table 1) require separate input files (NETCDF format),
353 as model-data comparison for these two scenarios are run separately in ATAT. Table 1 and further references
354 (Hughes et al., 2011; 2016; Small et al., 2017), provide information regarding identification of the stratigraphic
355 setting of these two glaciological events as considered by ATAT. ATAT requires that geochronological data
356 (advance or deglacial) are interpolated onto the same grid projection and resolution as the ice-sheet model before
357 use. Though an imperfect solution to the problem of comparing grids of different resolution, (Section 2.3; Table
358 2), this was preferred to the alternative solution of regriding an ice sheet model onto a higher resolution grid, as
359 this may introduce the false impression of high resolution modelling sensitive to boundary conditions (e.g.
360 topography) beyond the actual model resolution.

361 Preparation of the geochronological data to be the same format and grid resolution as the ice sheet model output
362 requires use of a GIS software package such as ESRI ArcMap or QGIS. Users must define deglacial/advance ages
363 based either upon the availability of geochronological data in a cell, or based upon an empirical reconstruction
364 (Figure 4). These ages must be calibrated to a calendar which is the same as that output by the ice-sheet model (in
365 our case the 365-day calendar in units of seconds since 1-1-1). Where there are no data (i.e. outside the ice-sheet
366 limit), the grid value must be kept at 0. When multiple dates are contained within a cell, expert judgement is
367 required to ascertain which date is most representative of the deglaciation of a region. This assessment should be
368 based upon the quality of sample taken; criteria for establishing this quality are considered in Small et al. (2017).
369 In the case where a profile of dates has been collected (for example up a vertical section at the side of a valley, or
370 from multiple depths of a marine core) the date which most closely defines the timing of final deglaciation of an
371 area should be chosen, as this is the focus of ATAT. The assembly of this geochronological database input into
372 ATAT should consider the reliability of ages, removing outliers and unreliable ages (see Small et al. (2017) for a
373 discussion of this issue). In particular, loose constraints, such as cosmogenic dates which display inheritance or
374 radiocarbon dates effected by a depositional hiatus, should be removed as this have the potential to bias results.

375 In a comparable manner, the attribution of error to each cell is also reliant upon expert interpretation. The
376 magnitude of error may vary between the source of geochronological data (radiocarbon, cosmogenic nuclide or
377 luminescence) and user choice for experimental design (e.g. 1, 2 or 3 sigma). A single error value must be given
378 for each dated cell, corresponding to the maximum threshold beyond which the user deems it is unacceptable for
379 a model prediction to occur (Figure 3). Given that creating this input data may involve many expert decisions (e.g.
380 which date has the relevant stratigraphic setting, which date(s) are most reliable?), this part of the process is not
381 yet automated within ATAT. This data preparation stage is therefore the most time-consuming and user-intensive
382 part of the process. However, users only need to define the data-based advance/deglacial grid once to compare to
383 multiple model outputs. Future work should consider alternatives means of choosing dates and identifying outliers,
384 such as Bayesian age modelling (e.g. Chivverell et al., 2013). The input data NetCDF file should also contain the
385 variables latitude, longitude, base topography (the topography that the ice-sheet modelling is conducted on and
386 the elevation of the geochronological sample (Table 3).

387 ATAT is called from a suitable python command-line environment, using several system arguments to define
388 input variables (Table 1; Figure 5). Users must define whether they are testing a deglacial or advance scenario.

389 ATAT only considers the last time that ice advances over an area. Therefore, caution must be undertaken when
390 defining advance data in regions where multiple readvances occur, and users should consider limiting the time
391 interval of the ice sheet model tested when examining specific events (e.g. a well-dated readvance or ice sheet
392 build-up). The location of the file containing the geochronological data grid (e.g. Figure 5) is then required. From
393 this file, the age and error grids are converted to arrays. For the age data, null values are masked out using the
394 numpys masked array function. A second array that accounts for error is then created, the properties of which
395 depends upon whether a deglacial or advance scenario is being tested. For a deglacial scenario, a model prediction
396 will be unacceptable if the cell is ice-covered after the range of the date error is accounted for, but the cell may
397 become deglaciaded any time before this. Therefore, the associated error value is added onto the cell date, to create
398 a maximum age at which a cell must be deglaciaded by to conform to the ice sheet model (Figure 3). The opposite
399 is true for advance ages; ice can cover a cell any time after the date and associated error, but cannot cover the cell
400 before the date of the advance. In order to allow for advances which occur after the date and its error, associated
401 error is therefore subtracted from the date cell (Figure 3). To account for the uneven spatial distribution of dates,
402 a weighting for each date is then calculated based upon their spatial proximity. This weighting is used later when
403 comparing the data to the model output. To calculate this weighting (w_i), ATAT defines a local spatial density of
404 dated values based upon a kernel search of 10 neighbouring cells.

405 The user must define the path to the ice sheet model output, from which the modelled deglacial age will be
406 calculated and eventually compared to the data (Figure 4). The user must also define whether to base deglacial
407 timing on an ice thickness or grounded extent mask variable (Table 2). If the user selects thickness, the margin is
408 defined by an increase from 0 ice thickness. For the mask, the user is also asked to supply the number which refers
409 to grounded ice extent. The timing of advance is then determined by the change of a cell to this number (Figure
410 5). The margin position recreated by the ice-sheet model has a spatial uncertainty due to downscaling issues and
411 fluctuations which may occur between recorded outputs. To account for this, ATAT calculates a second set of
412 modelled deglacial ages, whereby the deglaciaded region at each modelled time output is expanded to all cells
413 which neighbour the originally identified deglaciaded or advanced over cells. Furthermore, the spatial resolution
414 of ice-sheet models typically means that the emergence of ice-free topography at the edge or within an ice-sheet
415 (e.g. in situations such as steep-sided valleys or nuntaks) are poorly represented. To account for this, ATAT firstly
416 calculates the modelled ice-sheet surface at each time output by adding ice thickness to the input base topography.
417 Where the modelled surface elevation is below that of the sample elevation, these cells are identified as being
418 deglaciaded (Figure 5). The downscaling of topography onto ice-sheet model grids also introduces a vertical
419 uncertainty. This is accounted for in ATAT through calculating the difference between sample elevation and the
420 reference elevation. A second metric which identifies cells as having been deglaciaded if they are also within this
421 vertical uncertainty is also calculated (Figure 5).

422 **3.2 Model-data comparison**

423 Once the required variables have been retrieved from the NETCDF data and manipulated, ATAT compares the
424 geochronological age and modelled age at each location (Figure 4). Firstly, the grid cells which have data are
425 categorised as to whether there is model-data agreement, based on the criteria shown in Figure 3. Since all dating
426 techniques only record the absence of ice, geochronological data provides only a one-way constraint on palaeo-
427 ice sheet activity. For deglacial ages, deglaciaded could occur any time before the geochronological data provided

428 and within the error of the date (i.e. deglacial ages are minimum constraints), but deglaciation must not occur after
429 the error of the date is considered (Figure 3). For advance ages, advance must have happened after the date or
430 within error beforehand (i.e. advance ages are maximum constraints), but palaeo-ice sheet advance cannot occur
431 in the time period before that dated error (Figure 3). Once ATAT has determined whether each cell conforms to
432 these criteria, a map is produced identifying at which locations the ice sheet model agrees with the
433 geochronological data.

434 Though the criteria described above and illustrated in Figure 3 allow for the identification of dates which conform
435 to the predictions of an ice sheet model, they provide little insight into how close the timing of the model prediction
436 is to the geochronological data. If these were the only criteria on which a model-data comparison was made, it
437 could prove problematic. In an extreme case, one could envisage that all retreat dates are adhered to by a model
438 run that deglaciates from a maximum extent implausibly rapidly (say 50 years!), and, given that we only have
439 one-way (minimum) constraints on deglaciation (Figure 3), this model run would conform to all modelled dates.
440 Whilst the nature of geochronological data (being only able to determine the absence of ice) does not preclude
441 such a scenario, this assumes that there is no inherent value to the expert judgement and stratigraphic interpretation
442 of each date as being close to palaeo-ice sheet timing (cf. Small et al. 2017). Therefore, ATAT also determines
443 the temporal proximity of the geochronological data and the model prediction. Firstly, a map of the difference
444 between modelled and empirical ages is created (Figure 5). This enables the identification of dates which are a
445 large distance away from the model prediction. Secondly, the route-mean square error (RMSE) is calculated using
446 the Eq. (2):

$$447 \quad RMSE = \sqrt{\frac{1}{n} \sum_{i=1}^n (g_i - m_i)^2},$$

448 (1)

449 where n is the number of cells which contain empirical geochronological information, g_i is the associated
450 geochronological date, and m_i is the model predicted age. The RMSE works well when the geochronological
451 data is evenly spatially distributed, either from a reconstruction (i.e. isochrones) or a wealth of dates. ATAT also
452 calculates a weighted RMSE (wRMSE), for situations where this is not the case (i.e. there is a paucity of dates
453 that are not distributed evenly across the domain) using Eq. (3):

$$454 \quad wRMSE = \sqrt{\frac{1}{n} \sum_{i=1}^n ((g_i - m_i)/w_i)^2},$$

455 (2)

456 where w_i is the spatial weighting factor. Results of the RMSE and wRMSE calculations are separated by the
457 degree to which included dates agree with model output. This creates an array of metrics with varying levels of
458 consideration of (Figure 5). Both the RMSE and wRMSE are calculated for all dates, to create a metric that doesn't
459 account for dating error but may give an indication of how close a model-run gets to dated cells, and also for those
460 dates which where model-data agreement within dating error occurs to create a metric which does account for
461 model-error (Figure 5). ATAT then produces a .csv file containing all calculated statistics per ice-sheet model
462 output file. We suggest that the most rigorous metric, the wRMSE of dates which conform within
463 geochronological data and model downscaling uncertainty (Figure 5), should most frequently used. However,
464 other metrics, such as the RMSE of all dates, may give an indication of performance earlier in the modelling

465 process. For example, initial results may reveal that no or very few dates conform to a set of model simulations
466 within model and data uncertainty, but the RMSE of all dates may give an indication of models and associated
467 parameters to be explored further. Given the complexity of data-model comparison, different statistics may have
468 different uses. For instance, the percentage of covered dates may prove useful to identify the worst performing
469 model runs (i.e. the bottom 50%), whilst the wRMSE of dates within error may be more convenient for choosing
470 between model runs. However, given the uncertainty in ice-sheet modelling it is likely that in an ensemble there
471 will be no single model run which has significantly better metrics than others, so ATAT may best be used to
472 choose members which pass a user-defined threshold of combined metrics.

473 Pragmatically, we envisage that ATAT could be used in the following ways, though others may exist. In sensitivity
474 experiments (e.g. Huybrechts, 1990; Hubbard et al., 2009; Patton et al., 2016), ATAT could be used to quantify
475 how the alteration of a parameter influences the fit of a model to geochronological data. In ensemble experiments,
476 ATAT could be used to rank the performance of individual ensemble member simulations with respect to
477 geochronological constraints, either as a means of ruling out simulations with the poorest performance (e.g.
478 Gregoire et al., 2012) or calibrating input parameters for further experiments (e.g. Tarasov et al., 2012). Where
479 the results of an ensemble experiment have been amalgamated (i.e. where each cell has a distribution of ice-free
480 ages), ATAT could be compared to measures of average modelled deglaciation/advance age and against standard
481 deviations of these. Such comparisons could reveal areas of persistent model-data mismatch. If this is the case,
482 this may form the basis of identifying regions of significant model uncertainty (does this site not match due to
483 poor implementation of processes in the model?) or form the basis for re-examination of the geological evidence
484 (are there reasons why this site is consistently an outlier?). Furthermore, ATAT could be used to explore how
485 incorporating additional processes into a model alter the fit to data. Here, we envisage two sets of model
486 experiments, one which includes a new implementation of a process in a model and another which does not
487 implement this process, whilst holding all other things equal between the two experiments. ATAT could then be
488 used to distinguish whether a better fit to geochronological data can be made when the new process is accounted
489 for.

490 **4. Application of tool**

491 **4.1 Ice Sheet Model**

492 To trial ATAT we used geochronological data and ice sheet modelling experiments from the former British-Irish
493 Ice Sheet (BIIS). A vast quantity of previous research has produced a high density of dates (Hughes et al., 2011)
494 which are being substantially augmented by the BRITICE-CHRONO project ([http://www.britice-
495 chronology.group.shef.ac.uk/](http://www.britice-chronology.group.shef.ac.uk/)). Along with an abundance of well documented landforms (Clark et al., 2017), this
496 makes the BIIS a data-rich study area for empirical reconstructions and ice sheet modelling. Ongoing modelling
497 work aims to capture the behaviour of the BIIS inferred from the geomorphological and geochronological record
498 (see Clark et al., 2012 for a recent reconstruction). We do not expect our model to capture these specific details.
499 Instead, the purpose of modelling in this paper is merely to illustrate the use of ATAT. We therefore restrict
500 ourselves to simplified modelling experiments and show only three model runs (Experiments A, B and C), whereas
501 a full ensemble experiment would contain hundreds or thousands of simulations.

502 Ice sheet modelling experiments were conducted using the Parallel Ice Sheet Model (PISM; Winkelmann et al.,
503 2011). This is a hybrid SIA-SSA model, with an implementation of grounding line physics. It is therefore suited
504 to modelling both the marine-based portions of the BIIS and the terrestrial realm. The model simulates the history
505 of the BIIS from 40 ka to present. The model is run at 5 km resolution, with basal topography derived from the
506 General Bathymetric chart of the Oceans (www.gebco.net). This is updated to account for isostatic adjustment
507 using a viscoelastic Earth model (Bueler et al., 2007) and a scalar eustatic sea level offset based on the SPECMAP
508 data (Imbrie et al., 1984). All three model runs, labelled A-C, had the same input parameters and boundary
509 conditions, apart from climate forcing. We take a similar approach to Seguinot et al. (2016) in computing a climate
510 forcing. Modern values of temperature and precipitation are perturbed by a proxy temperature record, in this case
511 the GRIP ice core record (Johnsen et al., 1995). These are input into a positive degree day model to calculate mass
512 balance (Calov and Greve, 2005). Input precipitation values are the same between experiments. To introduce
513 variation between the experiments, temperature varies such that Experiment A is the equivalent of modern day
514 values, Experiment B has values uniformly reduced by 1°C and Experiment C has values uniformly reduced by
515 2°C. All other parameters and forcings are equal between experiments. This simple approach to climate forcing
516 here used for demonstration purposes only, and does not capture the changes to atmospheric and oceanic
517 circulation patterns that occur during a glacial cycle.

518 The maximum extent of ice for each experiment is shown in Figure 6 and the timing of advance and retreat is
519 shown in Figure 7. Potentially unrealistic ice sheets occur in the North Sea, perhaps due to the choice of domain
520 not including the influence of the Fennoscandian ice sheet in this area. As noted above, we do not expect these
521 model runs to fully replicate the reconstructed characteristics of the BIIS (e.g. Clark et al., 2012). However, it is
522 worth noting general, visually-derived, observations regarding the outputs shown in Figure 6. For larger
523 temperature offsets, the ice sheet gets bigger, the timing of maximum extent gets progressively later and the
524 modelled ice sheet gets thicker (Figure 6). In all experiments, there is generally a gradual advance toward the
525 maximum extent followed by retreat (Figure 7). This pattern is interrupted by a later readvance that corresponds
526 to the timing of the Younger Dryas in the GRIP record; this causes ice to regrow over high elevation areas such
527 as Scotland and central Wales. The extent of this readvance increases with decreased temperature offsets between
528 experiments (Figure 7). Smaller readvances, occurring around 16.5 ka also occur (Figure 7).

529 **4.2 Geochronological data**

530 Ice-sheet advance dates were taken from the compilation of Hughes et al. (2016) and gridded to the ice sheet
531 model domain (Figure 4). In total, 61 cells were represented with advance dates (Figure 8A). Considering now
532 ice-sheet retreat (Figure 8B), dates deemed reliable or probably reliable by Small et al. (2017) were used (i.e.
533 those given a ‘traffic light rating’ of green or amber). For the dated advance and retreat locations, the
534 geochronological data in each cell was assigned an error corresponding to that which was reported in the literature.
535 We also compared our results to the ‘likely’ empirical reconstruction of Hughes et al. (2016), based on that of
536 Clark et al. (2012) (Figure 8C), using the minimum and maximum bounding envelopes to assign an error to each
537 cell of the ice sheet grid (Figure 8D). The largest errors occur in the North Sea region, where there is a lack of
538 empirical data (e.g. Figures 8A and B).

539 4.3 Results

540 Table 4 shows selected statistics derived by ATAT when comparing the three ice-sheet modelling experiments
541 (Figures 6 and 7) against the three categories of data (Advance, Retreat, Isochrones; Figure 8). wRMSE was not
542 calculated for the DATED isochrone reconstruction, as grid points are distributed evenly and therefore have equal
543 spatial weighting (Table 4). Experiment C produces modelled ice-sheets with the greatest areal extent, and
544 therefore performs best at correctly covering the dated areas (Table 4). However, none of the three experiments
545 perform particularly well when compared with the data or the empirical reconstruction regarding timing and
546 results in high (>2000 year) RMSEs (Table 4). The application of ATAT and the results from these simplified
547 experiments allow us to suggest directions for analysing future experiments.

548 All three experiments produced large RMSEs, in the order of thousands of years, when compared to all three
549 categories of data (Table 4). For advance ages, the three simulations conform to a large number of dated locations
550 (e.g. 72% of ages in Experiments B and C; Table 4). However, the RMSEs of advance ages are high (Table 4).
551 This shows that, while the models perform well at matching the constraint of covering an area in ice after an
552 advance age (Figure 3), the models often glaciates a region much later than required. Advance dates are particularly
553 difficult to obtain from the stratigraphic record, and often there may be a long hiatus between the initial deposition
554 of datable material and the subsequent advance of a glacier. Future experiments with large ensembles should
555 therefore consider the number of advance dates conformed to (rather than the RMSE) as a more robust guide for
556 model performance during ice advance.

557 For the retreat comparisons, the three modelling experiments conform to a larger percentage of sites, seemingly
558 outperforming the empirically-derived DATED reconstruction (Table 4). However, where model-data agreement
559 occurs, the RMSE produced are much higher when the model is compared to the DATED reconstruction. This is
560 due to the reconstruction containing large uncertainties in regions which lack geochronological control (for
561 example in the North Sea, Figure 8). These uncertainties, a product of spatial interpolation across regions with
562 sparse information, are much greater than those associated with individual dates. Figure 9A shows examples of
563 output maps from ATAT which display the spatial pattern of agreement and the magnitude of the difference
564 between Experiment C and the DATED reconstruction. This shows that due to the uncertainty associated with
565 North Sea glaciation, even where the model produces an unrealistic artefact, there is data-model agreement.
566 Furthermore, ATAT produces a map which displays the number of years between data-based and modelled retreat
567 and/or advance (e.g. Figure 9B). Figure 9B, which compares Experiment C to the DATED isochrones, shows that
568 the timing of model-data disagreement is spatially variable. If more modelling simulations were conducted, such
569 maps may reveal regions of reconstruction or particular dates which are difficult to simulate in the model. In such
570 cases, data or model re-evaluation may be required and herein lies the potential utility of this ATAT tool in making
571 sense of ensemble model runs. However, such model-data comparison awaits a full-ensemble simulation which
572 accounts for model uncertainty (e.g. Hubbard et al., 2009).

573 5. Summary and concluding remarks

574 Here we present ATAT, an automated timing-accordance tool for comparing ice-sheet model output with
575 geochronological data and empirical ice sheet reconstructions. We demonstrate the utility of ATAT through three
576 simplified simulations of the former British-Irish Ice Sheet. Note that a larger ensemble model of hundreds to

577 thousands of runs is required for model evaluation (e.g. Hubbard et al., 2009). ATAT enables users to quantify
578 the difference between the simulated timing of ice sheet advance and retreat and those from a chosen dataset, and
579 allows production of cumulative ice coverage agreement maps that should help distinguish between less and more
580 promising runs. We envisage that this tool will be especially useful for ice-sheet modellers through justifying
581 model choice from an ensemble, quantifying error and tuning ice-sheet model experiments to fit geochronological
582 data. Ideally, this tool should be used in combination with other evaluation methods, such as fit to relative sea-
583 level records. In the case where locations or regions of data cannot be fit by a model, and all model uncertainty
584 has been accounted for in an ensemble simulation, the comparisons made in ATAT may also highlight that data
585 re-evaluation is necessary. ATAT is supplied as supplementary material to this article.

586 **6. Code Availability**

587 ATAT 1.1 source code is freely distributed under a GNU GPL licence as supplementary material to this paper and
588 can be downloaded from <https://figshare.com/s/38d0fd268684ad0fcc2d>. An example geochronological data grid
589 can also be downloaded as supplementary material. The ice sheet modelling experiments shown here were
590 conducted using the Parallel Ice Sheet Model (<http://pism-docs.org/>). Development of PISM is supported by
591 NASA grant NNX17AG65G and NSF grants PLR-1603799 and PLR-1644277. The geochronological data used
592 is freely available from <https://www.sciencedirect.com/science/article/pii/S0012825216304408#s0105> and
593 <https://doi.pangaea.de/10.1594/PANGAEA.848117>.

594 **6.1. General Instructions**

595 ATAT is written in python, and distributed as both .py script, for use in Python 2, and a .py3 script, for use with
596 Python 3. The tool requires installation of Python and the following freely available Python packages:

- 597 • netCDF4 (<https://pypi.python.org/pypi/netCDF4>)
- 598 • numpy (<http://www.numpy.org/>)
- 599 • scipy (<https://www.scipy.org/>)
- 600 • matplotlib (<https://matplotlib.org/>)
- 601 • matplotlib toolkit basemap (<https://matplotlib.org/basemap/>)

602 ATAT can be run from any Python enabled environment (e.g. IDLE, BASH). Here we provide the following
603 simple instructions for running ATAT in a BASH shell. For numerous runs, a shell script should be created.

604 From the command line, launch the ATAT script using python (“python ATATv1.1.py”). Eight command-line
605 arguments (A1 - A8), separated by a space should then follow.

606 A1 dictates whether deglacial or advance ages are being tested. Type “DEGLACIAL” or “ADVANCE”
607 accordingly.

608 A2 is the path to the geochronological data file (e.g. “/home/ATAT/geochron.nc”)

609 A3 defines whether the model extent is based on thickness or a mask. Type THK or MSK accordingly.

610 A4 is the path to the ice-sheet model output file (e.g. “/home/ATAT/icesheetmodel1.nc”)

611 A5 is the value of the ice-sheet output mask. A value is required even if A3 = THK, but can be any value as it will
612 be ignored.

613 A6 to A8 control output maps. A6 defines whether the output map should consider margin uncertainty, with a
614 value of BORDER or NONE.

615 A7 defines whether the model-data offset map displaces RMSE (option “NONE”) or wRMSE (“WEIGHTED”).

616 A8 specifies which dates are plotted on the difference map, and can be “ALL” for all dates, “COVERED” for
617 those which at some point were covered by ice and “INERROR” to display only those dates where model-data
618 agreement within dating error occurred.

619 An example command would be “python ATATv1.1.py DEGLACIAL /home/ATAT/dated_recon.nc MSK
620 /home/ATAT/experiment1.nc 2 BORDER WEIGHTED INERROR”. ATAT then outputs the two maps and a csv
621 table containing all derived statistics.

622 Input geochronological data can be created in a GIS environment such as ArcMap or QGIS. Here, the user must
623 discern the appropriate geochronological data for each grid cell. Since geochronological data is usually stored as
624 point data, this must be gridded to single grid points as positive values, with surrounding areas of no data assigned
625 a value of 0. When comparing to a reconstruction (e.g. Hughes et al., 2016), cells outside the reconstruction
626 should be assigned a value of 0. Those within the reconstruction should be assigned a value corresponding to the
627 reconstructed age of retreat. The gridded data must be converted to NetCDF format, the details of which are shown
628 in Table 3. We emphasise that the quality of geochronological data used must be considered, and an example of
629 how to filter geochronological data is documented in Small et al. (2017). Ice thickness grids can be created using
630 ice sheet modelling software such as PISM (Winkelmann et al., 2011). The two grids (data and model) must be
631 aligned and have the same size dimensions for use in ATAT. Examples are included as supplementary material,
632 including a model output from Ely et al. (in review).

633 *Acknowledgements:* This work was supported by the Natural Environment Research Council consortium grant;
634 BRITICE-CHRONO NE/J009768/1. Development of PISM is supported by NASA grant NNX17AG65G and
635 NSF grants PLR-1603799 and PLR-1644277. We thank Evan Gowan and Lev Tarasov for their constructive
636 reviews which improved the manuscript.

637 **References**

638 Auriac, A., Whitehouse, P.L., Bentley, M.J., Patton, H., Lloyd, J.M. and Hubbard, A. Glacial isostatic adjustment
639 associated with the Barents Sea ice sheet: a modelling inter-comparison. *Quaternary Science Reviews*, 147, 122-
640 135, 2016.

641 Applegate, P.J., Kirchner, N., Stone, E.J., Keller, K. and Greve, R. An assessment of key model parametric
642 uncertainties in projections of Greenland Ice Sheet behavior. *Cryosphere*, 6(3), 589-606, 2012.

643 Arnold, J.R. and Libby, W.F. Radiocarbon dates. *Science*, 113(2927), 111-120, 1951.

644 Balco, G. Contributions and unrealized potential contributions of cosmogenic-nuclide exposure dating to glacier
645 chronology, 1990–2010. *Quaternary Sci Rev*, 30(1), 3-27, 2011.

646 Bamber, J.L. and Aspinall, W.P.. An expert judgement assessment of future sea level rise from the ice sheets. *Nat*
647 *Clim Change*, 3(4), 424-427, 2013.

648 Bateman, M.D., Evans, D.J., Roberts, D.H., Medialdea, A., Ely, J. and Clark, C.D., The timing and consequences
649 of the blockage of the Humber Gap by the last British– Irish Ice Sheet. *Boreas*. 47(1), 41-61, 2018.

650 Boulton, G. and Hagdorn, M. Glaciology of the British Isles Ice Sheet during the last glacial cycle: form, flow,
651 streams and lobes. *Quaternary Sci Rev*, 25(23), 3359-3390, 2006.

652 Braconnot, P., Harrison, S.P., Kageyama, M., Bartlein, P.J., Masson-Delmotte, V., Abe-Ouchi, A., Otto-Bliesner,
653 B. and Zhao, Y., 2012. Evaluation of climate models using palaeoclimatic data. *Nature Climate Change*, 2(6),
654 417-424, 2012.

655 Briggs, R.D. and Tarasov, L. How to evaluate model-derived deglaciation chronologies: a case study using
656 Antarctica. *Quaternary Sci Rev*, 63, 109-127, 2013.

657 Briggs, R.D., Pollard, D. and Tarasov, L. A data-constrained large ensemble analysis of Antarctic evolution since
658 the Eemian. *Quaternary Sci Rev*, 103, 91-115, 2014.

659 Brown, E.J., Rose, J., Coope, R.G. and Lowe, J.J. An MIS 3 age organic deposit from Balglass Burn, central
660 Scotland: palaeoenvironmental significance and implications for the timing of the onset of the LGM ice sheet in
661 the vicinity of the British Isles. *J Quaternary Sci*, 22(3), 295-308, 2007.

662 Bueler, E.D., Lingle, C.S. and Brown, J. Fast computation of a viscoelastic deformable Earth model for ice-sheet
663 simulations. *Ann Glaciol*, 46(1), 97-105, 2007.

664 Bueler, E. and Brown, J. Shallow shelf approximation as a “sliding law” in a thermomechanically coupled ice
665 sheet model. *J Geophys Res-Earth*, 114(F3), 2009.

666 Calov, R. and Greve, R. A semi-analytical solution for the positive degree-day model with stochastic temperature
667 variations. *J Glaciol*, 51(172), 173-175, 2005.

668 Chiverrell, R.C., Thrasher, I.M., Thomas, G.S., Lang, A., Scourse, J.D., van Landeghem, K.J., Mccarroll, D.,
669 Clark, C.D., Cofaigh, C.Ó., Evans, D.J. and Ballantyne, C.K. Bayesian modelling the retreat of the Irish Sea Ice
670 Stream. *J Quaternary Sci*, 28(2), 200-209, 2013.

671 Clark, C.D., Hughes, A.L., Greenwood, S.L., Jordan, C. and Sejrup, H.P. Pattern and timing of retreat of the last
672 British-Irish Ice Sheet. *Quaternary Sci Rev*, 44, 112-146, 2012.

673 Cornford, S.L., Martin, D.F., Graves, D.T., Ranken, D.F., Le Brocq, A.M., Gladstone, R.M., Payne, A.J., Ng,
674 E.G. and Lipscomb, W.H. Adaptive mesh, finite volume modeling of marine ice sheets. *Journal of Computational
675 Physics*, 232(1), 529-549, 2013.

676 DeConto, R.M. and Pollard, D. Contribution of Antarctica to past and future sea-level rise. *Nature*, 531(7596),
677 591-597, 2016.

678 Duller, G.A.T. Single grain optical dating of glacial deposits. *Quaternary Geochronology*, 1(4), 296-304, 2006.

679 Dyke, A.S. An outline of North American deglaciation with emphasis on central and northern Canada.
680 *Developments in Quaternary Sciences*, 2, 373-424, 2004.

681 Dyke, A.S. An outline of North American deglaciation with emphasis on central and northern Canada.
682 *Developments in Quaternary Sciences*, 2, 373-424, 2004.

683 Edwards, T.L., Fettweis, X., Gagliardini, O., Gillet-Chaulet, F., Goelzer, H., Gregory, J.M., Hoffman, M.,
684 Huybrechts, P., Payne, A.J., Peregó, M. and Price, S. Effect of uncertainty in surface mass balance-elevation
685 feedback on projections of the future sea level contribution of the Greenland ice sheet. *Cryosphere*, 8(1), 195-208.
686 2014.

687 [Ely, J.C., Clark, C.D., Hindmarsh, R.C.A., Hughes, A.L.C., Greenwood, S.L., Bradley, S.L., Gasson, E., Gregoire,](#)
688 [L., Gandy, N., Stokes, C.R. and Small, D. An approach to combining geomorphological and geochronological](#)

689 [data with ice sheet modelling, demonstrated using the last British-Irish Ice Sheet. *Journal of Quaternary Science*.](#)
690 [In review.](#)

691 Fowler, A.C. A sliding law for glaciers of constant viscosity in the presence of subglacial cavitation. In
692 Proceedings of the Royal Society of London A: Mathematical, Physical and Engineering Sciences, 407(1832),
693 147-170, 1986.

694 Fretwell, P., Pritchard, H.D., Vaughan, D., Bamber, J.L., Barrand, N.E., Bell, R., Bianchi, C., Bingham, R.G.,
695 Blankenship, D.D., Casassa, G. and Catania, G. Bedmap2: improved ice bed, surface and thickness datasets for
696 Antarctica. *Cryosphere*, 7, 375-393, 2013.

697 Fuchs, M. and Owen, L.A. Luminescence dating of glacial and associated sediments: review, recommendations
698 and future directions. *Boreas*, 37(4), 636-659, 2008.

699 Gasson, E., DeConto, R.M., Pollard, D. and Levy, R.H. Dynamic Antarctic ice sheet during the early to mid-
700 Miocene. *Proceedings of the National Academy of Sciences*, 113(13), 3459-3464, 2016.

701 Golledge, N.R., Levy, R.H., McKay, R.M., Fogwill, C.J., White, D.A., Graham, A.G., Smith, J.A., Hillenbrand,
702 C.D., Licht, K.J., Denton, G.H. and Ackert, R.P. Glaciology and geological signature of the Last Glacial
703 Maximum Antarctic ice sheet. *Quaternary Sci Rev*, 78, 225-247, 2013.

704 Gomez, N., Pollard, D., Mitrovica, J.X., Huybers, P., Clark, P.U. Evolution of a coupled marine ice sheet-sea
705 level model, *J Geophys Res*, 117, F01013, 2012.

706 Gomez, N., Pollard, D. and Mitrovica, J.X. A 3-D coupled ice sheet–sea level model applied to Antarctica through
707 the last 40 ky. *Earth and Planet Sc Lett*, 384, 88-99, 2013.

708 Gowan, E.J. An assessment of the minimum timing of ice free conditions of the western Laurentide Ice Sheet.
709 *Quaternary Sci Rev*, 75, 100-113, 2013.

710 Gregoire, L.J., Payne, A.J. and Valdes, P.J. Deglacial rapid sea level rises caused by ice-sheet saddle collapses.
711 *Nature*, 487(7406), 219-222, 2012.

712 Greve, R. and Hutter, K. Polythermal three-dimensional modelling of the Greenland ice sheet with varied
713 geothermal heat flux. *Ann. Glaciol.*, 21, 8-12, 1995.

714 [Greve, R., Wyrwoll, K.H. and Eisenhauer, A. Deglaciation of the Northern Hemisphere at the onset of the Eemian
715 and Holocene. *Ann. Glaciol.*, 28, 1-8, 1999.](#)

716 Gudmundsson, G.H., Krug, J., Durand, G., Favier, L. and Gagliardini, O. The stability of grounding lines on
717 retrograde slopes. *Cryosphere*, 6, 1497-1505, 2012.

718 Gudmundsson, G.H. Ice-shelf buttressing and the stability of marine ice sheets, *Cryosphere*, 7, 647-655, 2013.

719 Heroy, D.C. and Anderson, J.B. Radiocarbon constraints on Antarctic Peninsula ice sheet retreat following the
720 Last Glacial Maximum (LGM). *Quaternary Sci Rev*, 26(25), 3286-3297, 2007.

721 Heyman, J., Stroeven, A.P., Harbor, J.M. and Caffee, M.W. Too young or too old: evaluating cosmogenic
722 exposure dating based on an analysis of compiled boulder exposure ages. *Earth Planet Sc Lett*, 302(1), 71-80,
723 2011.

724 Hindmarsh, R.C. Consistent generation of ice- streams via thermo- viscous instabilities modulated by membrane
725 stresses. *Geophys Res Lett*, 36(6). 2009.

726 Hubbard, A., Bradwell, T., Golledge, N., Hall, A., Patton, H., Sugden, D., Cooper, R. and Stoker, M. Dynamic
727 cycles, ice streams and their impact on the extent, chronology and deglaciation of the British–Irish ice sheet.
728 *Quaternary Sci Rev*, 28(7), 758-776, 2009.

729 Hughes, A.L., Greenwood, S.L. and Clark, C.D. Dating constraints on the last British-Irish Ice Sheet: a map and
730 database. *J Maps*, 7(1), 156-184, 2011.

731 Hughes, A.L., Clark, C.D. and Jordan, C.J. Flow-pattern evolution of the last British Ice Sheet. *Quaternary Sci*
732 *Rev*, 89, 148-168, 2014.

733 Hughes, A.L., Gyllencreutz, R., Lohne, Ø.S., Mangerud, J. and Svendsen, J.I. The last Eurasian ice sheets—a
734 chronological database and time- slice reconstruction, DATED- 1. *Boreas*, 45(1), 1-45, 2016.

735 Hughes, T.J., Is the West Antarctic ice sheet disintegrating? *J. Geophys. Res.*, 78 (33), 7884-7910, 1973.

736 [Huybrechts, P. The Antarctic ice sheet during the last glacial-interglacial cycle: a three-dimensional](#)
737 [experiment. *Ann. Glaciol.* 14, 115-119, 1990.](#)

738 Imbrie, J., Hays, J.D., Martinson, D.G., McIntyre, A., Mix, A.C., Morley, J.J., Pisias, N.G., Prell, W.L.,
739 Shackleton, N.J. The orbital theory of Pleistocene climate: support from a revised chronology of the marine $\delta^{18}O$
740 record. In: Berger, A., Imbrie, J., Hays, H., Kukla, G., Saltzman, B. (Eds.), *Milankovitch and Climate, Part I. D.*
741 Reidel Publishing, Dordrecht, 269–305, 1984.

742 Johnsen, S.J., Dahl-Jensen, D., Dansgaard, W. and Gundestrup, N. Greenland palaeotemperatures derived from
743 GRIP bore hole temperature and ice core isotope profiles. *Tellus B*, 47(5), 624-629, 1995.

744 Kirchner, N., Hutter, K., Jakobsson, M. and Gyllencreutz, R. Capabilities and limitations of numerical ice sheet
745 models: a discussion for Earth-scientists and modelers. *Quaternary Sci Rev*, 30(25), 3691-3704, 2011.

746 Kirchner, N., Ahlkrone, J., Gowan, E.J., Lötstedt, P., Lea, J.M., Noormets, R., von Sydow, L., Dowdeswell, J.A.
747 and Benham, T. Shallow ice approximation, second order shallow ice approximation, and full Stokes models: A
748 discussion of their roles in palaeo-ice sheet modelling and development. *Quaternary Sci Rev*, 147, 136-147, 2016.

749 Kleman, J., Hättestrand, C., Stroeven, A.P., Jansson, K.N., De Angelis, H. and Borgström, I. Reconstruction of
750 Palaeo- Ice Sheets- Inversion of their Glacial Geomorphological Record. In Knight, P.G. (Eds) *Glacier science*
751 *and environmental change*, 192-198, 2006.

752 Larour, E., Seroussi, H., Morlighem, M. and Rignot, E. Continental scale, high order, high spatial resolution, ice
753 sheet modeling using the Ice Sheet System Model (ISSM). *J Geophys Res-Earth*, 117(F1), 2012.

754 Libby, W.F., Anderson, E.C. and Arnold, J.R. Age determination by radiocarbon content: world-wide assay of
755 natural radiocarbon. *Science*, 109(2827), 227-228, 1949.

756 Lingle, C.S. and Clark, J.A. A numerical model of interactions between a marine ice sheet and the solid earth:
757 Application to a West Antarctic ice stream. *J Geophys Res-Oceans*, 90(C1), 1100-1114, 1985.

758 Livingstone, S.J., Cofaigh, C.Ó., Stokes, C.R., Hillenbrand, C.D., Vieli, A. and Jamieson, S.S. Antarctic palaeo-
759 ice streams. *Earth-Sci Rev*, 111(1), 90-128, 2012.

760 Lorenz, E.N. Deterministic Nonperiodic Flow, *J. Atmos. Sci.*, 20, 130-141, 1963.

761 Lowe, J.J. and Walker, M.J. Radiocarbon Dating the Last Glacial-Interglacial Transition (Ca. 14–9 14C Ka Bp)
762 in Terrestrial and Marine Records: The Need for New Quality Assurance Protocols. *Radiocarbon*, 42(1), 53-68,
763 2000.

764 Lowell, T.V., Fisher, T.G., Hajdas, I., Glover, K., Loope, H. and Henry, T. Radiocarbon deglaciation chronology
765 of the Thunder Bay, Ontario area and implications for ice sheet retreat patterns. *Quaternary Sci Rev*, 28(17), 1597-
766 1607, 2009.

767 Lukas, S., Spencer, J.Q., Robinson, R.A. and Benn, D.I. Problems associated with luminescence dating of Late
768 Quaternary glacial sediments in the NW Scottish Highlands. *Quaternary Geochron*, 2(1), 243-248, 2007.

769 Mercer, J.H. West Antarctic ice sheet and CO₂ greenhouse effect: a threat of disaster. *Nature*, 271, 321-325, 1978.

770 Napieralski, J., Harbor, J. and Li, Y. Glacial geomorphology and geographic information systems. *Earth-Sci Rev*,

771 85(1), 1-22, 2007.

772 Ó Cofaigh, C.Ó. and Evans, D.J. Radiocarbon constraints on the age of the maximum advance of the British–Irish

773 Ice Sheet in the Celtic Sea. *Quaternary Sci Rev*, 26(9), 1197-1203, 2007.

774 Patton, H., Hubbard, A., Andreassen, K., Winsborrow, M. and Stroeven, A.P. The build-up, configuration, and

775 dynamical sensitivity of the Eurasian ice-sheet complex to Late Weichselian climatic and oceanic forcing.

776 *Quaternary Sci Rev*, 153, 97-121, 2016.

777 Pattyn, F. Sea-level response to melting of Antarctic ice shelves on multi-centennial timescales with the fast

778 Elementary Thermomechanical Ice Sheet model (f. ETISh v1. 0). *Cryosphere*, 11(4), p.1851-1878, 2017.

779 Pattyn, F., Perichon, L., Aschwanden, A., Breuer, B., De Smedt, B., Gagliardini, O., Gudmundsson, G.H.,

780 Hindmarsh, R., Hubbard, A., Johnson, J.V. and Kleiner, T. Benchmark experiments for higher-order and full

781 Stokes ice sheet models (ISMIP-HOM). *Cryosphere*, 2(1), 111-151, 2008.

782 Pattyn, F., Schoof, C., Perichon, L., Hindmarsh, R.C.A., Bueler, E., Fleurian, B.D., Durand, G., Gagliardini, O.,

783 Gladstone, R., Goldberg, D. and Gudmundsson, G.H. Results of the marine ice sheet model intercomparison

784 project, MISMIP. *Cryosphere*, 6(3), 573-588, 2012.

785 Pollard, D. and DeConto, R.M. Modelling West Antarctic ice sheet growth and collapse through the past five

786 million years. *Nature*, 458(7236), 329-332, 2009.

787 Ritz, C., Edwards, T.L., Durand, G., Payne, A.J., Peyaud, V. and Hindmarsh, R.C. Potential sea-level rise from

788 Antarctic ice-sheet instability constrained by observations. *Nature*, 528(7580), 115-118, 2015.

789 Robinson, A., Calov, R. and Ganopolski, A. Greenland ice sheet model parameters constrained using simulations

790 of the Eemian Interglacial. *Clim Past*, 7(2), 381-396, 2011.

791 [Rougier, J., 2007. Probabilistic inference for future climate using an ensemble of climate model](#)

792 [evaluations. *Climatic Change*, 81\(3-4\), pp.247-264.](#)

793 Rutt, I.C., Hagdorn, M., Hulton, N.R.J. and Payne, A.J. The Glimmer community ice sheet model. *J. Geophys.*

794 *Res-Earth*, 114(F2), 2009.

795 Schoof, C.S. Ice sheet grounding line dynamics: steady states, stability and hysteresis. *J. Geophys. Res. Earth*

796 *Surf.*, 112, F03S28, 2007.

797 Schoof, C. Coulomb friction and other sliding laws in a higher-order glacier flow model. *Math Mod Meth Appl*

798 *S*, 20(01), 157-189, 2010.

799 Schoof, C. Marine ice sheet stability. *J. Fluid Mech.*, 698, 62-72, 2012.

800 Seddik, H., Greve, R., Zwinger, T., Gillet-Chaulet, F. and Gagliardini, O. Simulations of the Greenland ice sheet

801 100 years into the future with the full Stokes model Elmer/Ice. *J Glaciol*, 58(209), 427-440, 2012.

802 Seguinot, J., Rogozhina, I., Stroeven, A.P., Margold, M. and Kleman, J. Numerical simulations of the Cordilleran

803 ice sheet through the last glacial cycle. *Cryosphere*, 10, 639-664, 2016.

804 Simpson, M.J., Milne, G.A., Huybrechts, P. and Long, A.J. Calibrating a glaciological model of the Greenland

805 ice sheet from the Last Glacial Maximum to present-day using field observations of relative sea level and ice

806 extent. *Quaternary Sci Rev*, 28(17), 1631-1657, 2009.

807 Small, D., Clark, C.D., Chiverrell, R.C., Smedley, R.K., Bateman, M.D., Duller, G.A., Ely, J.C., Fabel, D.,

808 Medialdea, A. and Moreton, S.G. Devising quality assurance procedures for assessment of legacy

809 geochronological data relating to deglaciation of the last British-Irish Ice Sheet. *Earth-Sci Rev*, 164, 232-250,
810 2017.

811 Smedley, R.K., Glasser, N.F. and Duller, G.A.T. Luminescence dating of glacial advances at Lago Buenos Aires
812 (~ 46° S), Patagonia. *Quaternary Sci Rev*, 134, 59-73, 2016.

813 Smedley, R.K., Chiverrell, R.C., Ballantyne, C.K., Burke, M.J., Clark, C.D., Duller, G.A.T., Fabel, D., McCarroll,
814 D., Scourse, J.D., Small, D. and Thomas, G.S.P. Internal dynamics condition centennial-scale oscillations in
815 marine-based ice-stream retreat. *Geology*, 45(9), 787-790, 2017.

816 Stokes, C.R., Tarasov, L., Blomdin, R., Cronin, T.M., Fisher, T.G., Gyllencreutz, R., Hättestrand, C., Heyman, J.,
817 Hindmarsh, R.C., Hughes, A.L. and Jakobsson, M. On the reconstruction of palaeo-ice sheets: recent advances
818 and future challenges. *Quaternary Sci Rev*, 125, 15-49, 2015.

819 Tarasov, L. and Peltier, W.R. A geophysically constrained large ensemble analysis of the deglacial history of the
820 North American ice-sheet complex. *Quaternary Sci Rev*, 23(3), 359-388, 2004.

821 Tarasov, L., Dyke, A.S., Neal, R.M. and Peltier, W.R. A data-calibrated distribution of deglacial chronologies for
822 the North American ice complex from glaciological modeling. *Earth Planet Sc Lett*, 315, 30-40, 2012.

823 Tushingham, A.M. and Peltier, W.R. Validation of the ICE- 3G Model of Würm- Wisconsin Deglaciation using
824 a global data base of relative sea level histories. *J Geophys Res-Solid Earth*, 97(B3), 3285-3304, 1992.

825 Weertman, J. Stability of the junction of an ice-sheet and an ice-shelf. *J. Glaciol.* 13 (67), 3-11, 1974.

826 Winkelmann, R., Martin, M.A., Haseloff, M., Albrecht, T., Bueller, E., Khroulev, C. and Levermann, A. The
827 Potsdam parallel ice sheet model (PISM-PIK)-Part 1: Model description. *Cryosphere*, 5(3), 715-726, 2011.

828

829

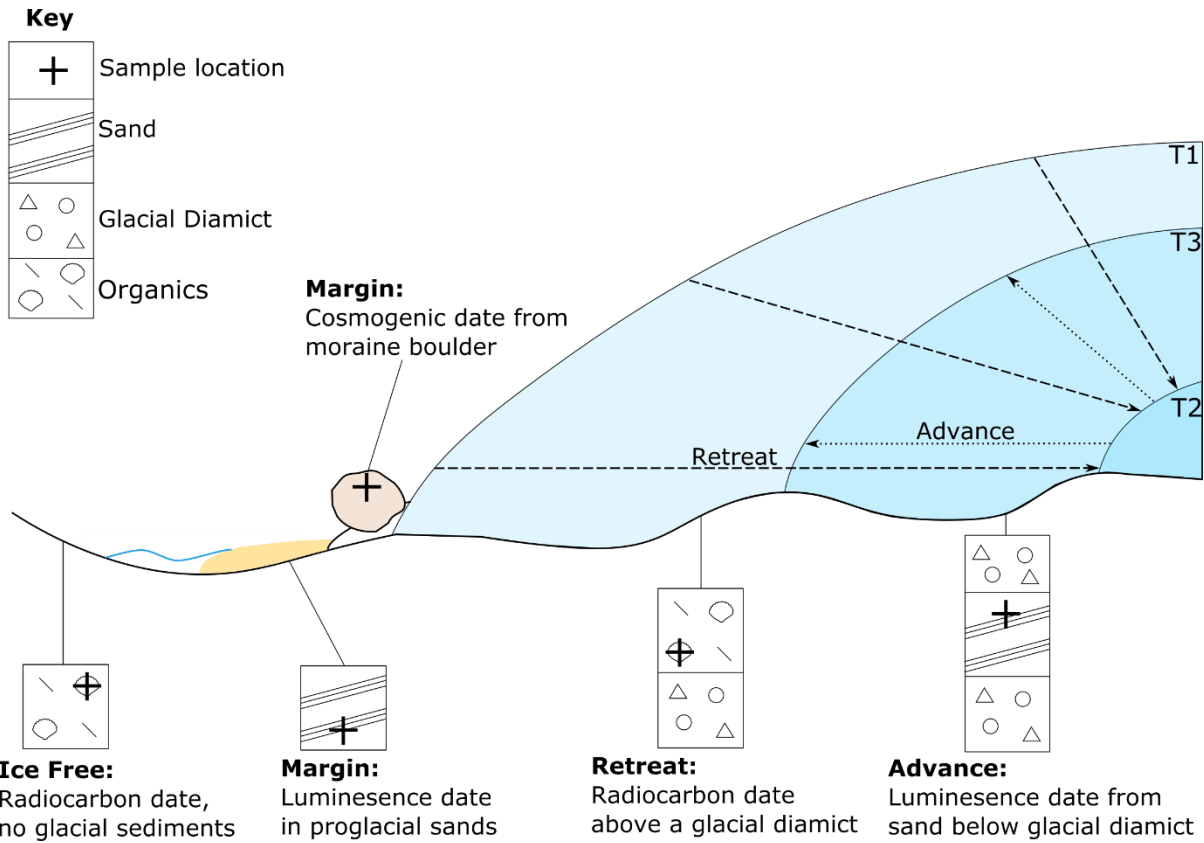
830

831

832

833

834

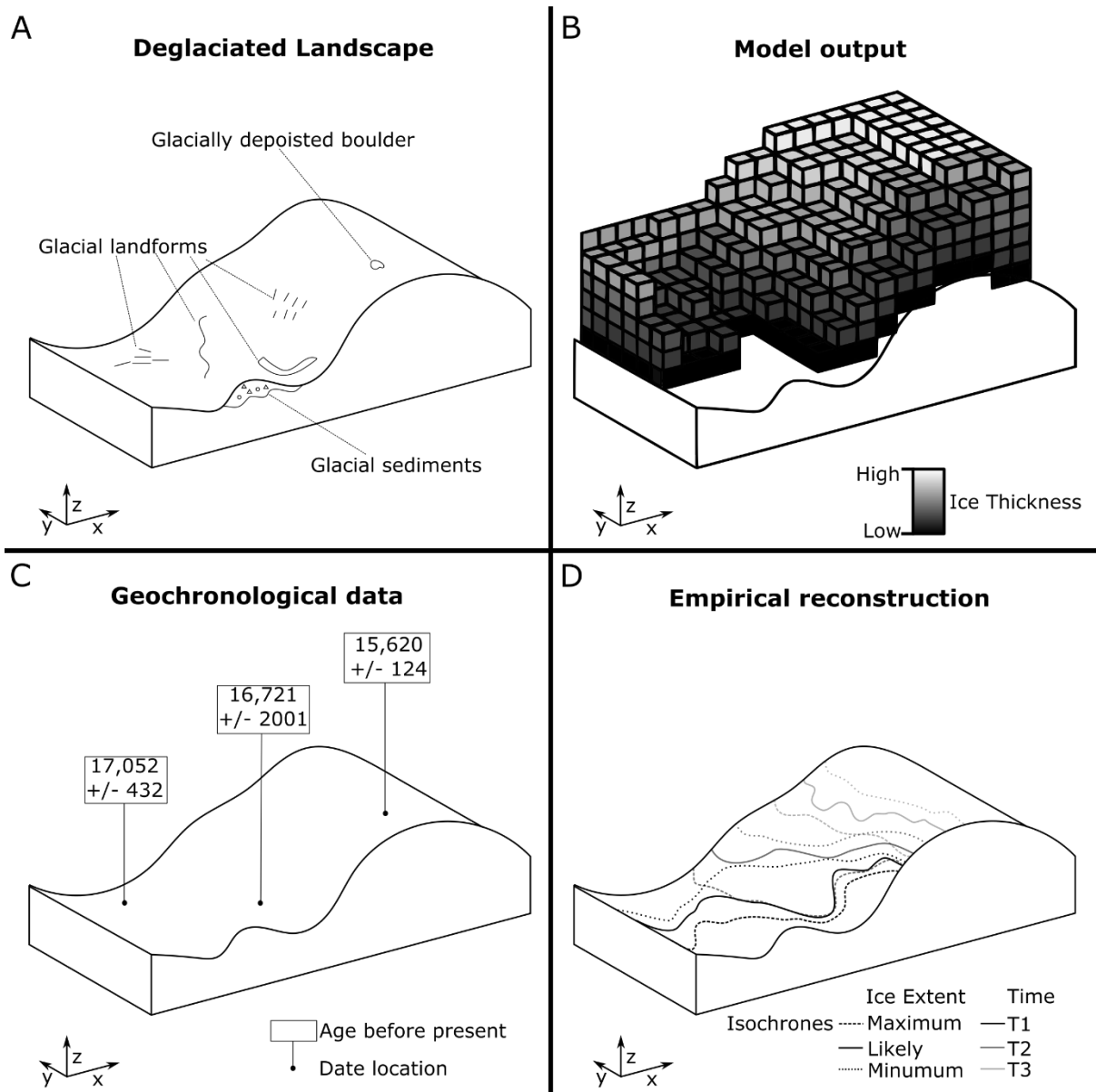


835

836

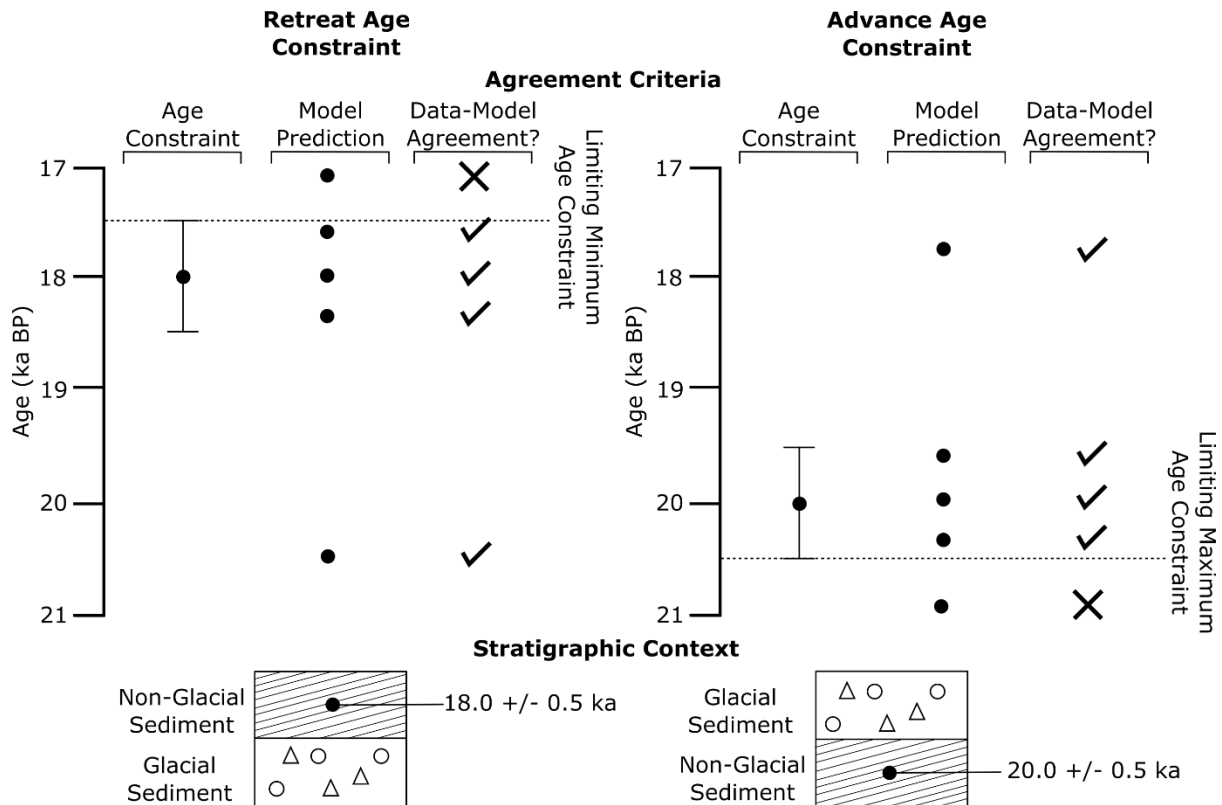
837

Figure 1: Schematic illustration of stratigraphic and inferred glaciological context of geochronological data. Note that at T1 the ice sheet is at its most advanced. It then retreats to a minimum at T2, before re-advancing to T3.



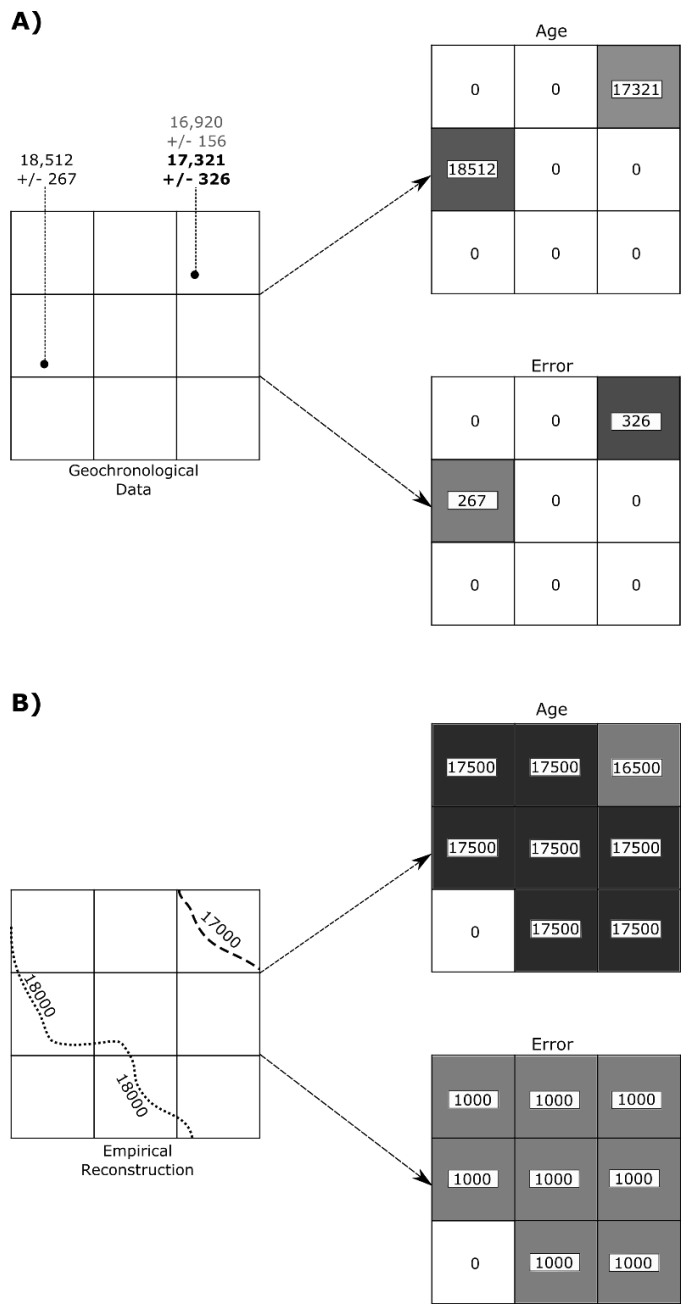
838

839 **Figure 2. Schematic of geochronological data and ice-sheet model output. A) A deglaciaded landscape,**
 840 **demonstrating some of the features used by palaeo-glaciologists when empirically reconstructing an ice**
 841 **sheet. B) Ice-sheet model output, displaying modelled ice-sheet thickness, in this case at a specific time. C)**
 842 **Geochronological data. D) Empirical reconstruction. Note how the nature of these data vary between**
 843 **source.**



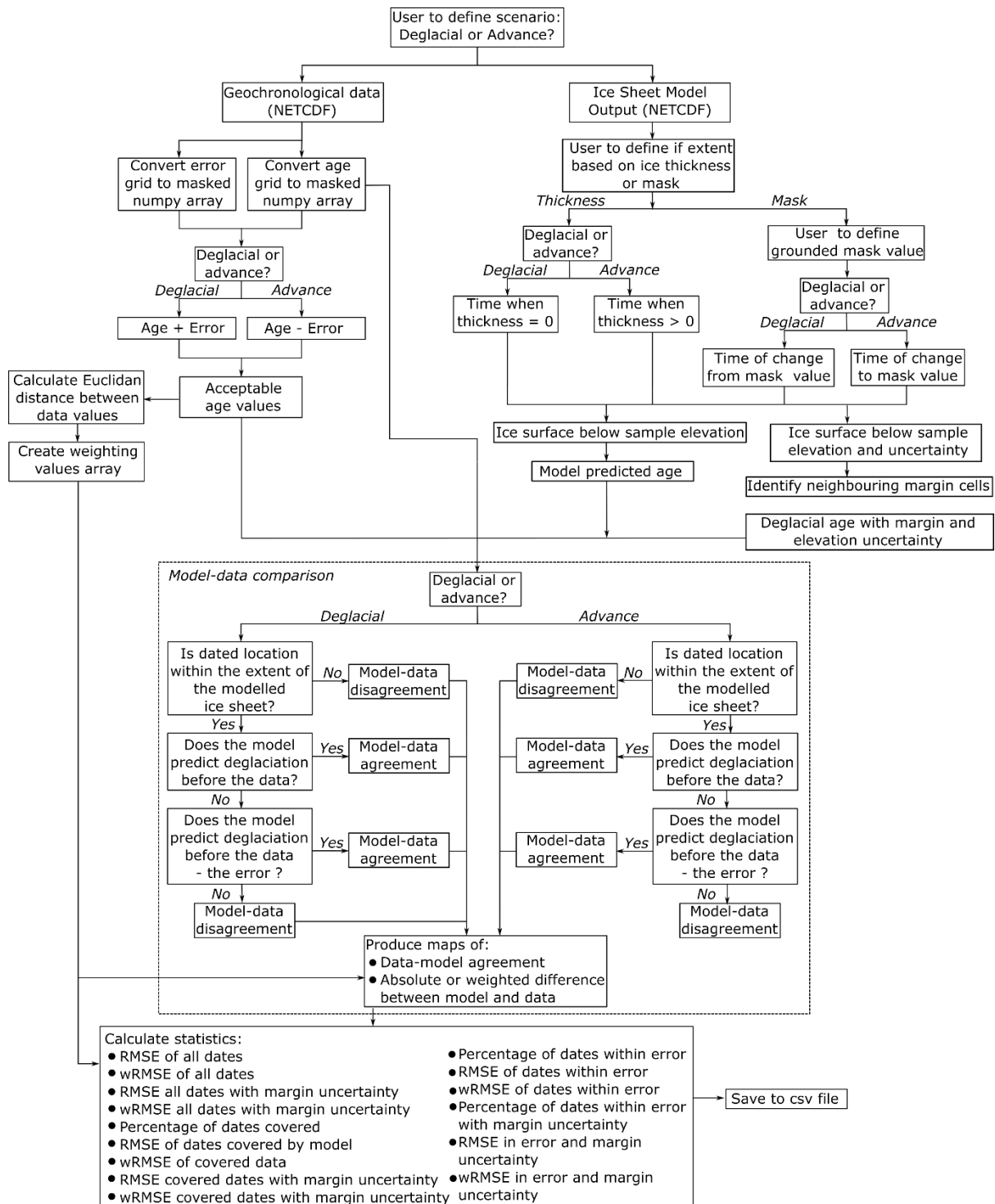
844

845 **Figure 3. Schematic of the identification of data-model agreement with consideration of error by ATAT**
 846 **for retreat (left) and advance (right) data. If a model predicts ice free conditions before an ice-free age, or**
 847 **during the associated error, there is data-model agreement. If deglaciation occurs at this location after the**
 848 **error, the model disagrees with the data. If a model predicts ice advance and cover before the advance age**
 849 **and its associated error, there is model-data disagreement. Agreement between the model and data occurs**
 850 **if ice advances over the location after the date, or before the date within the range of the error. This is used**
 851 **by ATAT to categorise sites as to whether agreement or disagreement between the model and data occurs.**



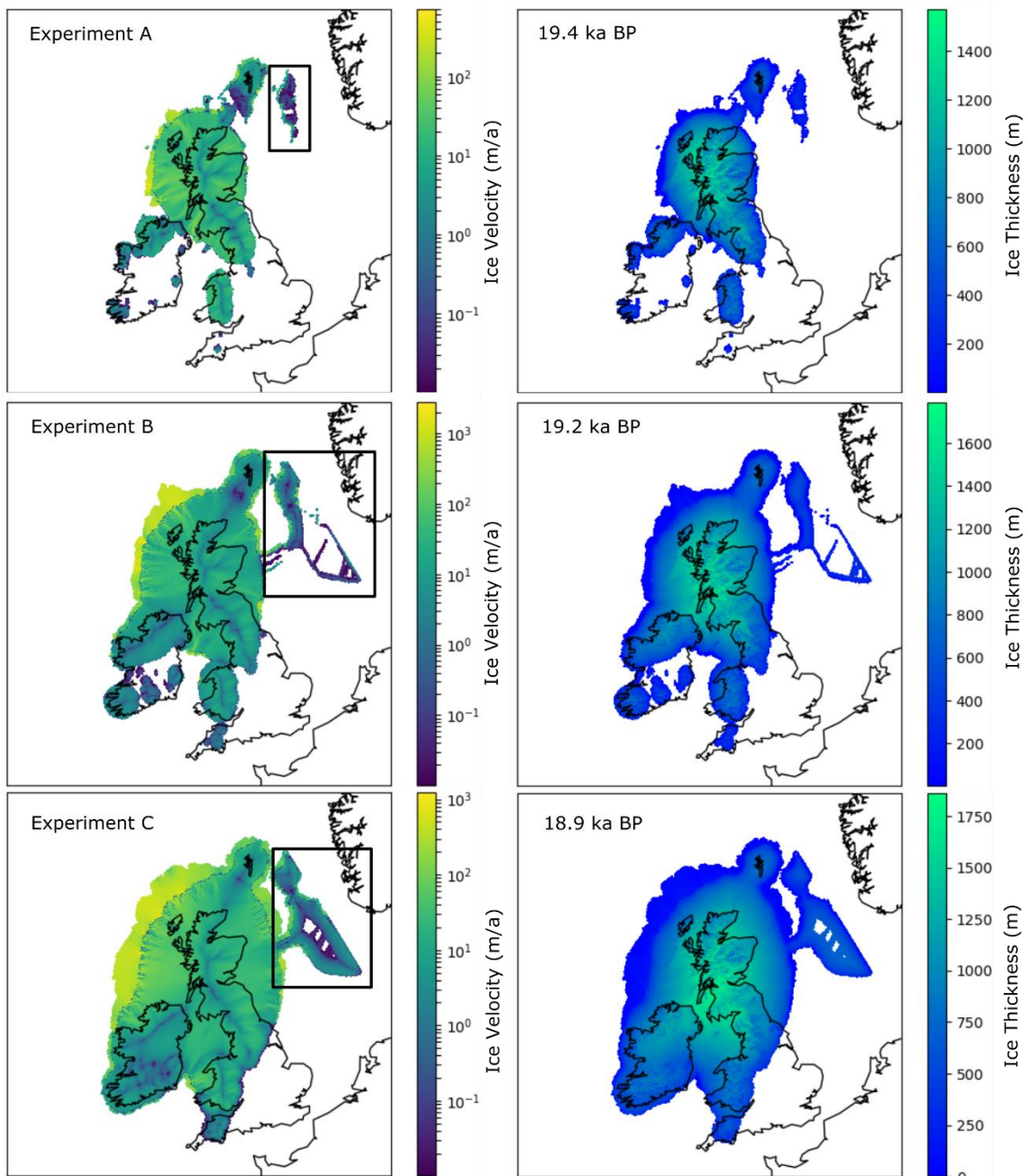
852

853 **Figure 4. Examples of empirical data preparation for ATAT. (A) Conversion of geochronological data into**
 854 **a grid for ATAT. In this example the user has made a judgement based on a priori knowledge that the date**
 855 **of $17,321 \pm 326$ is most representative of the event of interest. Note that age and error are split into separate**
 856 **grids, and that no data regions are assigned a value of 0. (B) Conversion of an empirical reconstruction**
 857 **(margin isochrones) into a grid for ATAT. Here we simply assume that the area between isochrones became**
 858 **deglaciated between at the age between the two isochrones, and that associated error is 1000 years. More**
 859 **complex reconstructions (e.g. Hughes et al., 2016) may require different user-defined rules.**



860

861 **Figure 5. Flow chart of ATAT procedure. See text for further description.**



862

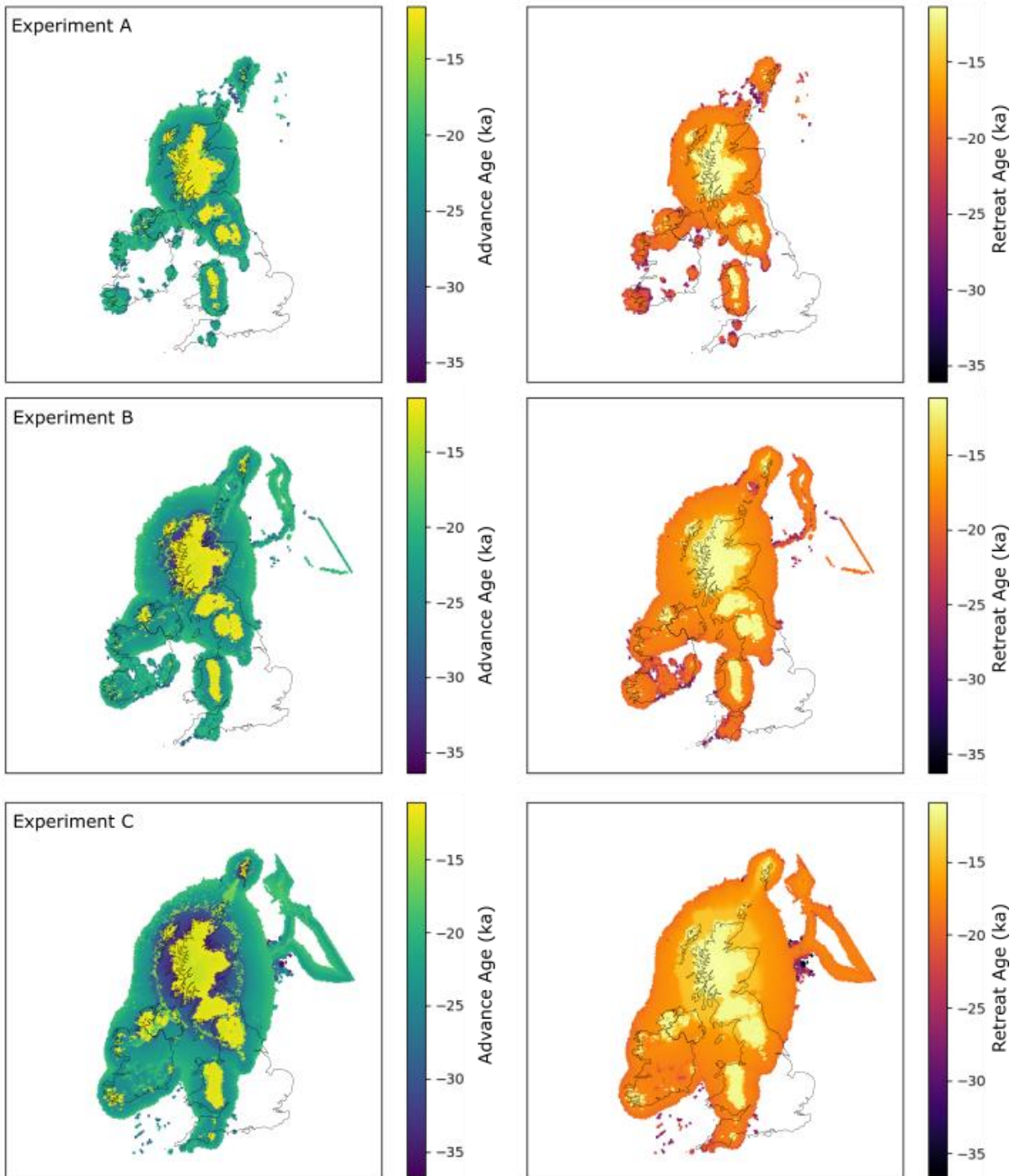
863

864

865

866

Figure 6. Maximum extent of produced ice sheet for the three experiments. Experiment B is 1°C colder than A, and experiment C is 2°C colder than A. Left panel shows ice velocity, right is ice thickness. The box on the left panel highlights likely erroneous output in the North Sea, likely a consequence of model domain, discussed further in the text.



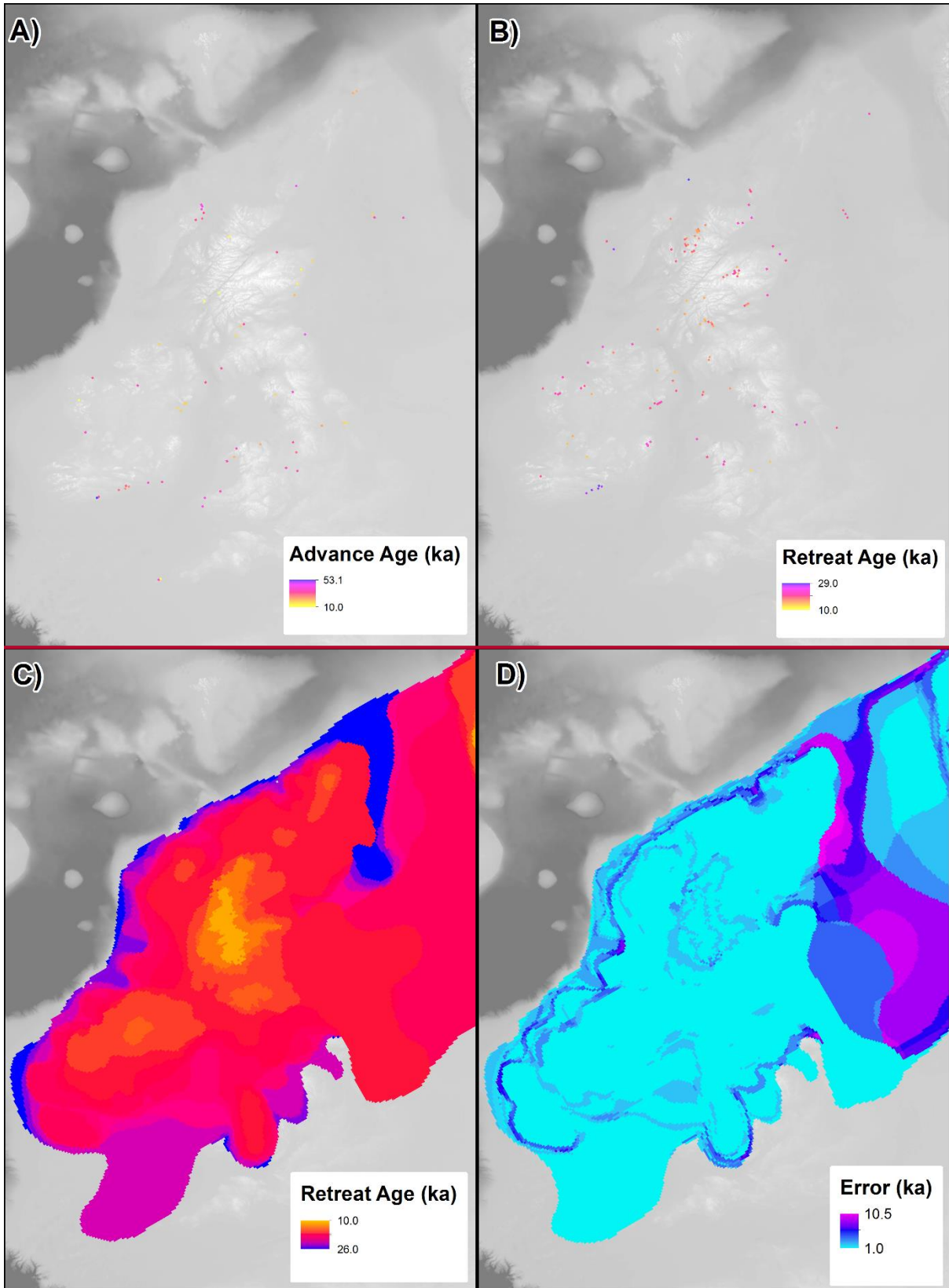
867

868

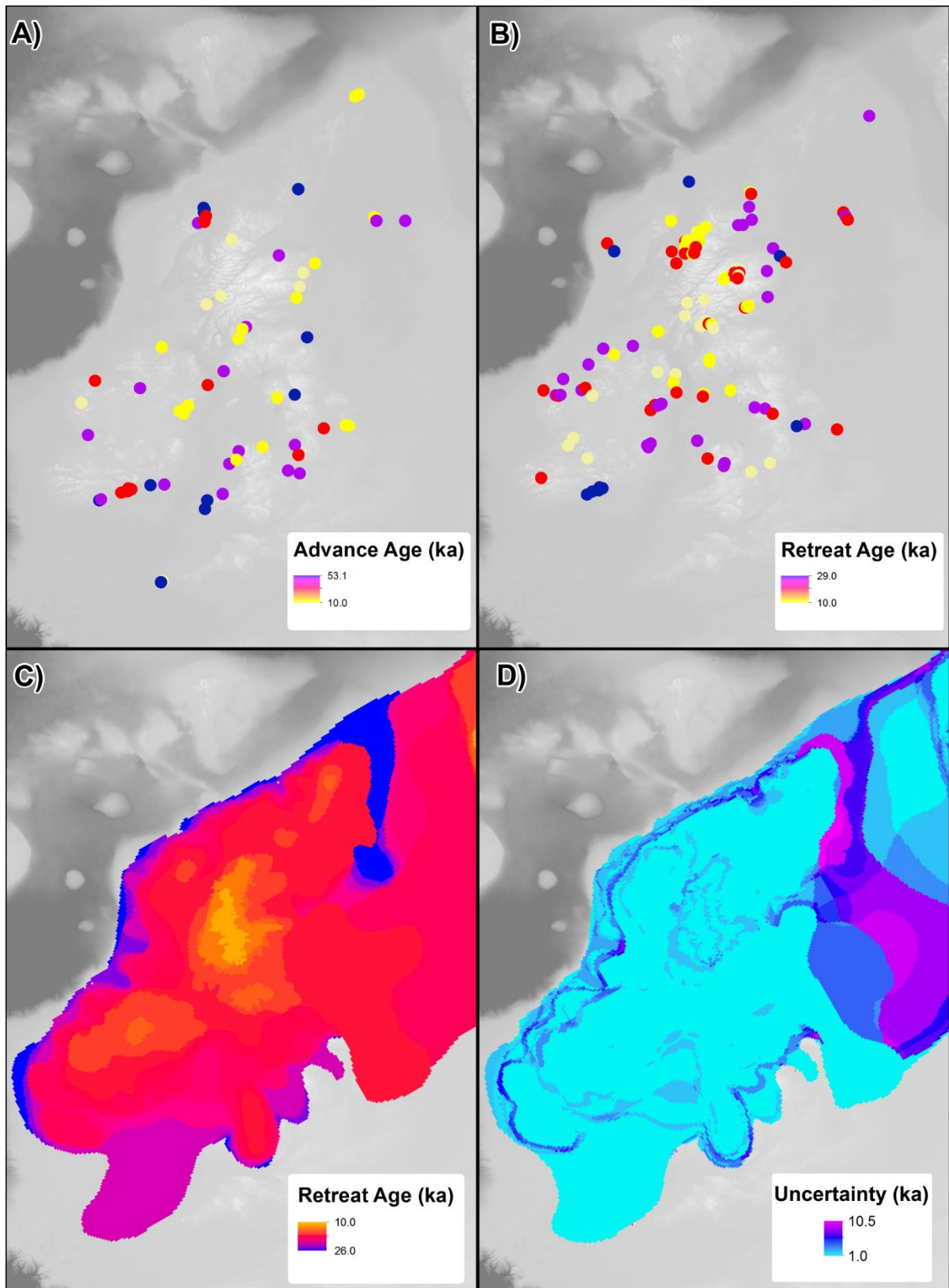
869

870

Figure 7. Timing of advance (left) and retreat (right) from the three ice sheet modelling experiments. Experiments are the same as in Figure 6. The early ages toward the centre of the model, and centred over higher topography, represent the modelled extent of the Younger Dryas readvance.

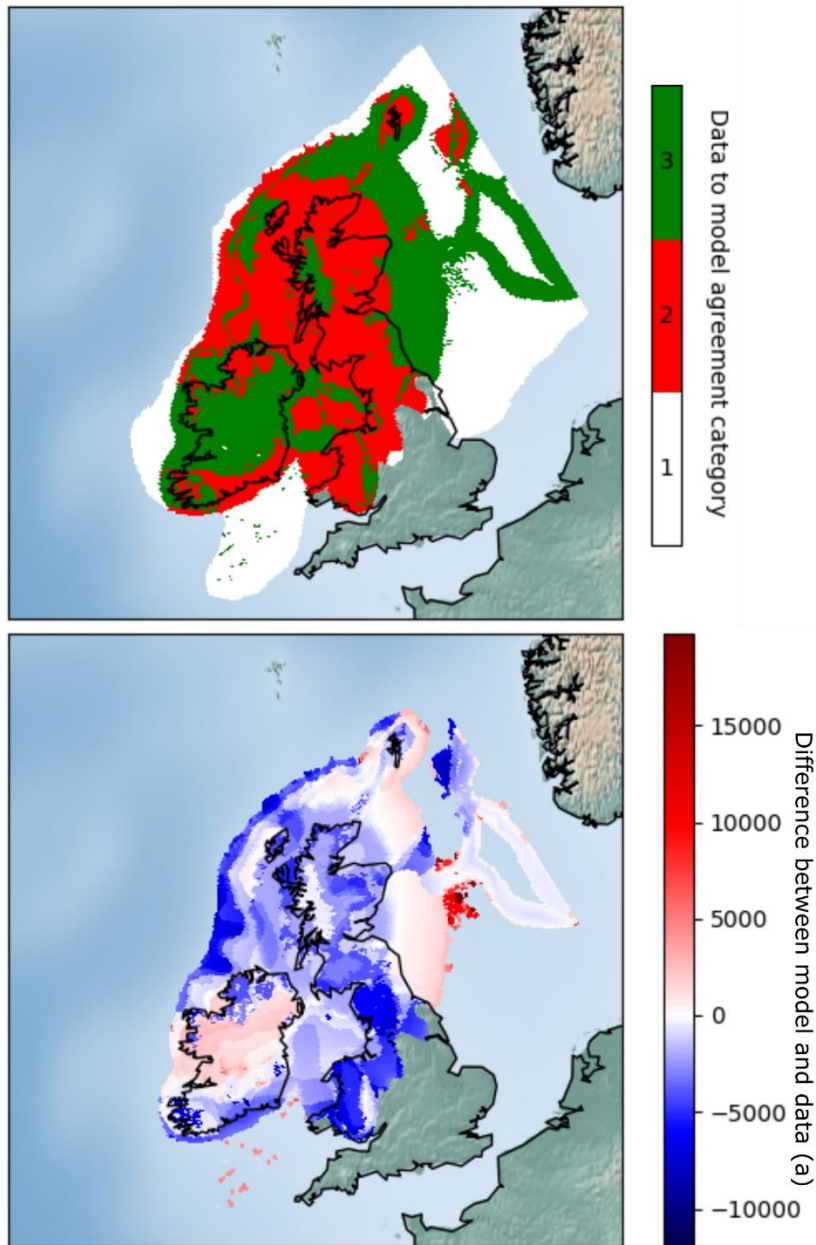


871



872

873 **Figure 8.** Example of geochronological data projected onto model raster grids; as point-data in A and B
 874 and from an empirical reconstruction in C and D. (A). Advance ages from Hughes et al. (2016). (B) Retreat
 875 ages from Small et al. (2017). (C) Retreat age derived from DATED isochrone reconstruction (Hughes et
 876 al., 2016). (D) Error associated with reconstruction in C.



877

878 **Figure 9.** Example mapped outputs from ATAT. In this case, experiment C was compared with the DATED
 879 reconstruction. Top map (cumulative agreement) shows categories of data-model agreement across the
 880 domain, where 1 = not covered by model, 2 = no agreement and 3 = data-model agreement within error.
 881 The lower map (model-data offset) shows magnitude of difference between model and data; negative values
 882 show a modelled retreat of ice later than the DATED isochrones, and positive values show a modelled
 883 retreat of ice before the DATED isochrones.

884 Table 1. Classification of geochronological data (after Hughes et al., 2011) and its use in ATAT.

Class	Glaciological context	Stratigraphic context	Example	Use in ATAT
Advance	Ice-sheet build up	Material directly below or incorporated within glacial diamict	Luminescence date from a sand below a glacial diamict	Ice cover a short time after this date
Retreat	Ice-free after ice cover	Dated material above glacial diamict	Radiocarbon date of a shell above a glacial diamict	Ice-free conditions from this date onwards (note deglaciation could have occurred a long time before)
Ice Free	Ice-free, but lacking direct information regarding ice	Dated material which indicates ice-free conditions but has no relation to ice cover. It may be much younger and not provide much useful constraint.	Radiocarbon date of organic sediments without underlying glacial sediments	
Margin	Proximal to an ice sheet margin	Dated material with information that ties it to an ice margin	Luminescence date in proglacial sands	
Exposure time (cumulative)	Length of time since sample exposed	N/A	Cosmogenic isotope on erratic boulder above a trimline	Not used

885

Table 2. Comparison of attributes between geochronological data and ice sheet model output.

	Nature of data produced	Spatial resolution	Spatial continuity	Temporal frequency and resolution	Sources of uncertainty	Main limitation
Geochronological data	Timing of the absence of ice at a location	Point location	Point location, unevenly distributed in space, but can be interpolated	Determined by data availability and associated error	Instrumental, environmental and stratigraphic factors	Reliant upon correct stratigraphic interpretation to tie to glaciological events
Ice-sheet model output	Simulation of physically plausible ice sheet conditions	Various, ranging from tens to unit kilometres.	Spatially even, regularly-spaced across entire domain	Continuous in time. Precise subannual resolution possible, but not recorded in practice	Parameterisations, boundary conditions	Based upon mathematical and physical approximations of ice flow

Data source	NetCDF Variable	Units	Dimensions	Description	Notes
		Time	unit x, y	Calendar years before present	
		before reference calendar date			
Ice sheet model output	thk	m	time, x,y	Ice thickness	Either “thk” or “msk” required by ATAT.
	msk	Integers	time, x,y	Grounded/floating/icefree mask	Either “thk” or “msk” required by ATAT. User defines value referring to the location of grounded ice
	lat	Decimal degrees	x, y	Latitude	
Both	lon	Decimal degrees	x, y	Longitude	
Geochronological data	age	Time	unit x, y	Timing of deglaciated conditions	Deglacial and advance ages must be in separate files.
		before reference calendar date			
	error	Seconds	x, y	Error associated with deglaciated conditions	Error associated with either deglacial and advance age must be in associated separate file.
	topg	m	x,y	Modern elevation at resolution of ice-sheet model	

elevation m x,y Elevation of collected sample

Table 3. Required input variables for ATAT NetCDF files.

Table 4: Example statistics from ATAT. Note that the RMSE is often altered by applying the spatial weighting to create wRMSE.

Ice Sheet Modelling Experiment	Advance			Retreat			Empirical Reconstruction; DATED		
	A	B	C	A	B	C	A	B	C
Percentage of dates covered	52.5	72.1	88.5	76.1	91.7	96.3	32.9	52.6	69.8
Percentage that agree within error	65.6	72.7	72.2	22.0	22.0	12.8	23.2	27.0	17.8
RMSE dates covered by model	11075.9	12732.7	13490.3	3879.0	4180.9	4945.4	2972.5	2678.0	2920.8
wRMSE dates covered by model	13357.3	13994.7	14849.7	4073.4	4450.3	5165.8	N/A	N/A	N/A
RMSE dates within error	655.7	478.6	289.3	403.6	259.7	236.2	12023.4	10638.7	8777.6
wRMSE dates within error	615.4	395.0	223.6	422.1	276.9	248.9	N/A	N/A	N/A